Biogeosciences, 22, 2667–2690, 2025
https://doi.org/10.5194/bg-22-2667-2025

Biogeosciences Open Access EGU

From the top: surface-derived carbon fuels greenhouse gas production at depth in a peatland

Alexandra Hedgpeth[1,2], Alison M. Hoyt[3], Kyle C. Cavanaugh[1], Karis J. McFarlane[2,★], and Daniela F. Cusack[1,4,5,★]

[1]Geography Department, University of California Los Angeles, Los Angeles, CA 94143, USA
[2]Center for Accelerator Mass Spectrometry, Lawrence Livermore National Laboratory, Livermore, CA 94550, USA
[3]Department of Earth System Science, Stanford University, Stanford, CA 94305, USA
[4]Department of Ecosystem Science & Sustainability, Colorado State University, Fort Collins, CO 80523, USA
[5]Smithsonian Tropical Research Institute, 0843-03092, Ancon, Panama, Republic of Panama
★These authors contributed equally to this work.

Correspondence: Alexandra Hedgpeth (hedgpea10@gmail.com)

Received: 29 April 2024 – Discussion started: 13 May 2024
Revised: 14 November 2024 – Accepted: 27 November 2024 – Published: 13 June 2025

Abstract. Tropical peatlands play an important role in global carbon (C) cycling, but little is known about factors driving carbon dioxide (CO_2) and methane (CH_4) emissions from these ecosystems, especially production in deeper soils. This study aimed to identify source material and processes regulating C emissions originating deep in three sites in a peatland on the Caribbean coast of Panama. We hypothesized that (1) surface-derived organic matter transported down the soil profile is the primary C source for respiration products at depth and that (2) high lignin content results in hydrogenotrophic methanogenesis as the dominant CH_4 production pathway throughout the profile. We used radiocarbon isotopic values to determine whether CO_2 and CH_4 at depth are produced from modern substrates or ancient deep peat, and we used stable C isotopes to identify the dominant CH_4 production pathway. Peat organic chemistry was characterized using ^{13}C solid-state nuclear magnetic resonance spectroscopy (^{13}C-NMR). We found that deep peat respiration products had radiocarbon signatures that were more similar to surface dissolved organic C (DOC) than deep solid peat. These results indicate that surface-derived organic matter was the dominant source for gas production at depth in this peatland, likely because of vertical transport of DOC from the surface to depth. Lignin, which was the most abundant compound (55 %–70 % of C), increased with depth across these sites, whereas other C compounds like carbohydrates did not vary with depth. These results suggest that there is no preferential decomposition of carbohydrates but instead preferential retention of lignin. Stable isotope signatures of respiration products indicated that hydrogenotrophic rather than acetoclastic methanogenesis was the dominant production pathway of CH_4 throughout the peat profile. These results show that deep C in tropical peatlands does not contribute greatly to surface fluxes of carbon dioxide, with compounds like lignin preferentially retained. This protection of deep C helps explain how peatland C is retained over thousands of years and points to the vulnerability of this C should anaerobic conditions in these wet ecosystems change.

1 Introduction

Climate change is expected to disturb hydrological cycles in the tropics, with changes in rainfall regimes already observed for many tropical regions (Barkhordarian et al., 2019; Feng and Fu, 2013; Barros et al., 2014; Duffy et al., 2022; Chadwick et al., 2016; Barkhordarian et al., 2019). Changes in rainfall are of particular relevance to the storage of the 70–130 Gt of organic carbon (OC) stored in tropical peatland soils under anaerobic conditions, which could be under threat of rapid mineralization if rainfall declines and aerobic conditions emerge (Girkin et al., 2022; Loisel et al., 2021). Tropical peatlands store the largest pool of vulnerable and irrecoverable C of any ecosystem type, and this pool is sequestered over thousands of years (Goldstein et al., 2020; Noon et al.,

2021). Despite their importance, tropical peatlands are logistically challenging environments to work in and are understudied compared to their northern counterparts, making tropical peatlands underrepresented in global C inventories (Ribeiro et al., 2021).

Peatlands sequester C as they build vertically with the oldest deposits at the base and less decomposed younger material accumulating at the surface (Clymo et al., 1998; Ingram, 1987). Despite temperatures ideal for microbial activity, the buildup of organic matter is possible because rates of primary production in the tropics exceed decomposition rates, which are low because peatland water tables are high (Nottingham et al., 2019; Page et al., 2011). Thus, deep peat is comprised of minimally processed plant material from the surface that accumulates due to anaerobic conditions, creating a globally significant buildup of C over time that could be metabolized if conditions became more favourable for decomposition (Hoyos-Santillan et al., 2019; Kettridge et al., 2015; Wilson et al., 2021). However, this age–depth relationship is not as straightforward in the tropics as in northern peatlands because tropical peatland microtopography shows higher variability due to increased vegetation diversity and size, and forest disturbance can have dramatic effects on peat accumulation patterns (Dommain et al., 2015; Girkin et al., 2019). The dominant vegetation that acts as the stabilizing structure in early peat development, as well as the vegetation that serves as the biological origin of the peat itself, is also different in northern and tropical peatlands, leading to differences in peatland development, organic chemistry, and accumulation patterns between these two regions (United Nations Environment Programme et al., 2008).

Under current conditions, there is considerable variation in C emissions across tropical wetland systems (Farmer et al., 2011; Fritts, 2022), but some relationships have been generally characterized. It is mostly accepted that water table depth (Cobb et al., 2017; Hoyos-Santillan et al., 2019; Hoyt et al., 2019), temperature (Girkin et al., 2020; Hirano et al., 2009; Jauhiainen et al., 2014), substrate availability, and associated links with the dominant vegetation type (Upton et al., 2018; Wright et al., 2011, 2013) are strong controls on surface emissions from tropical peatlands. Furthermore, surface vegetation plays an important role in peatland C cycling, both as the biological origin of the peat matrix, which is composed primarily of lignin-rich fibrous material in woody tropical peatlands, and via labile C inputs in the form of decomposing plant tissues or root exudates (Girkin et al., 2018; Lampela et al., 2014; Osaki et al., 2021). The majority of studies conducted in tropical peatlands have focused on the top 30 cm of the peat column; these depths are not only more accessible and easier to measure, but they are also assumed to contribute the majority of emissions (Dhandapani et al., 2022; Jauhiainen et al., 2005; Sjögersten et al., 2011). However, it is not known if the above drivers are mainly restricted to the surface or if these processes influence CO_2 and CH_4 production deeper within the peat profile.

In many peatlands, microbial respiration across the soil profile can be supported by multiple C sources, and it is possible to use the radiocarbon signature of C respired from peatlands to partition sources into modern or surface dissolved OC (DOC) transported down the soil profile versus older or buried solid C (Chanton et al., 2008; Hoyos-Santillan et al., 2016). Modern DOC, derived from surface vegetation, root exudates, and other recently photosynthesized organic matter, has a signature that is enriched in $\Delta^{14}C$. The existing peat and DOC from in situ decomposition of that deep peat would have depleted radiocarbon signatures compared to the modern DOC (Girkin et al., 2018; Wilson et al., 2016).

There have been several studies exploring the source of DOC used by microbes for respiration within peat soils. Most studies were from northern peatlands, and determined that respiration products were intermediate in their radiocarbon activity between newer surface DOC and older C in peat (Aravena et al., 1993; Chanton et al., 1995, 2008; Clymo et al., 1998; Corbett et al., 2013). Fewer studies have reported that respiration products are more similar to modern DOC radiocarbon signatures, demonstrating dominant use of surface DOC in deep peat gas production (Wilson et al., 2021). There is limited data from tropical peatlands, but two previous studies from the tropics found contrasting results; one found intermediate respiration products (i.e. produced by mixed sources) in a tropical peatland in Borneo (Hoyt, 2014), and another found modern surface-derived inputs are the dominant source in sites across the Pastaza-Marañon basin in Peru (Hoyt et al., 2020). Potential explanations for this variable source contribution in tropical peatlands include differences in hydrology across sites, as well as the difference in dominant vegetation across the tropics. Biological origin can influence the chemistry and bioavailability of both modern DOC inputs and the resulting older peat (Dhandapani et al., 2023; Gandois et al., 2014), which could contribute to the different results reported for these two tropical peatlands with distinct surface vegetation.

Methanogenesis is an important pathway of decomposition in wetland systems. Acetoclastic methanogenesis is associated with acetate fermentation and the production of CH_4 from relatively labile organic compounds, while hydrogenotrophic methanogenesis is associated with CO_2 reduction and can be supplied by the decomposition of more complex organic matter, with this second pathway being less energetically favourable to microbes (Kotsyurbenko et al., 2004; Sugimoto and Wada, 1993). Metabolically, acetoclastic methanogenesis is more energetically favourable (i.e. more potential energy released), more efficient in CH_4 production, and generally results in higher rates of CH_4 production compared to hydrogenotrophic methanogenesis (Kotsyurbenko et al., 2004; Liebner et al., 2015). Shifts in CH_4 production pathways between acetoclastic methanogenesis and hydrogenotrophic methanogenesis occur depending on substrate availability, with acetoclastic favoured if fermentation products are available, as has been seen with depth in

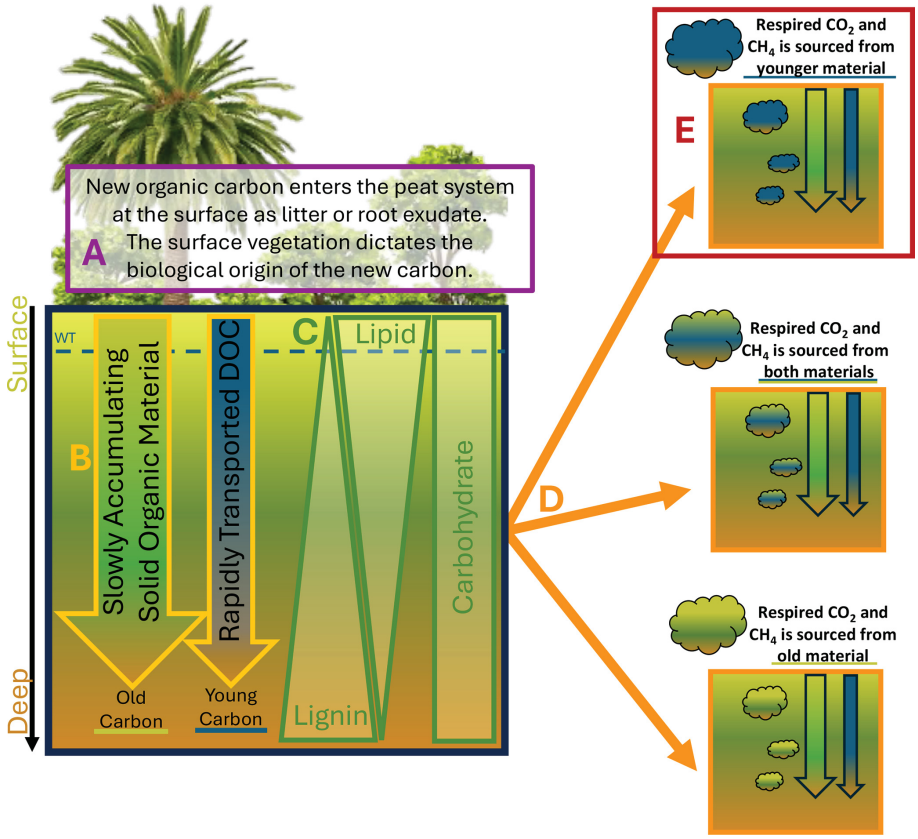

Figure 1. Schematic illustrating our conceptual understanding of the tropical peat C cycle. **(a)** Surface vegetation acts as the primary source of new organic material entering the peat system. Key contributors include dead plant matter and root exudates, and plant species influence the organic chemistry of these C inputs to soils. **(b)** Slow accumulation of solid peat matter (green) contrasts the rapid fluxes of fresh, modern dissolved organic carbon (DOC) from the surface (blue). **(c)** As bulk peat accumulates over time, decomposition impacts biochemical characteristics of solid peat down the soil profile through preferential preservation of lignin and loss of lipids while carbohydrate content remains constant. **(d)** Alternative scenarios are shown for gases produced within the peat soil, which exhibit C isotopic signatures that reflect the dominant source material or a combination of both sources. Both organic inputs can contribute to gas production – either from a single source (top orange box and bottom orange box) or a mix of both (middle orange box). **(e)** The results of this study indicate that the top scenario is most likely for these sites, with younger DOC fuelling belowground respiration and methanogenesis.

northern wetlands (Chanton et al., 2008; Corbett et al., 2013; Hornibrook et al., 2000). Changes in the availability of labile materials throughout the peat profile, even at depths of 2 m, may be crucial not only for supplying the C substrate for CO_2 and CH_4 production but also for influencing the mechanisms and quantities of CH_4 generated (Moore et al., 2013; Sun et al., 2012).

This study explored sources of soil surface C emissions, CH_4 production pathways, and organic C chemistry of peat in three sites in a peatland in Panama. Previous work suggested that subsurface peat may contribute substantially to net CO_2 and CH_4 flux from this peatland, but the source of C for these emissions was unclear (Wright et al., 2011). We used a combination of stable and radioisotope signatures of CO_2 and CH_4 and ^{13}C solid-state nuclear magnetic resonance spectroscopy (^{13}C-NMR) characterization of peat soils to identify the sources of the C gases produced in subsurface (> 30 cm) peat. We hypothesized that (i) surface-derived DOC is the primary C source for microbial respiration products at depth, where solid peat is more chemically complex and protected against decomposition. For this hypothesis, we predicted that deep solid peat would have a higher decomposition index compared with surface peat. We also hypothesize that (ii) hydrogenotrophic methanogenesis is the dominant CH_4 production pathway at depth, resulting from decomposition of complex organic matter, rather than fermentation of more simple C compounds, which would support acetoclastic methanogenesis (Fig. 1). We report and discuss radiocarbon analyses of subsurface DOC, CH_4, and CO_2 and peat biomolecular characterization using solid-state ^{13}C-NMR spectroscopy in a tropical peatland.

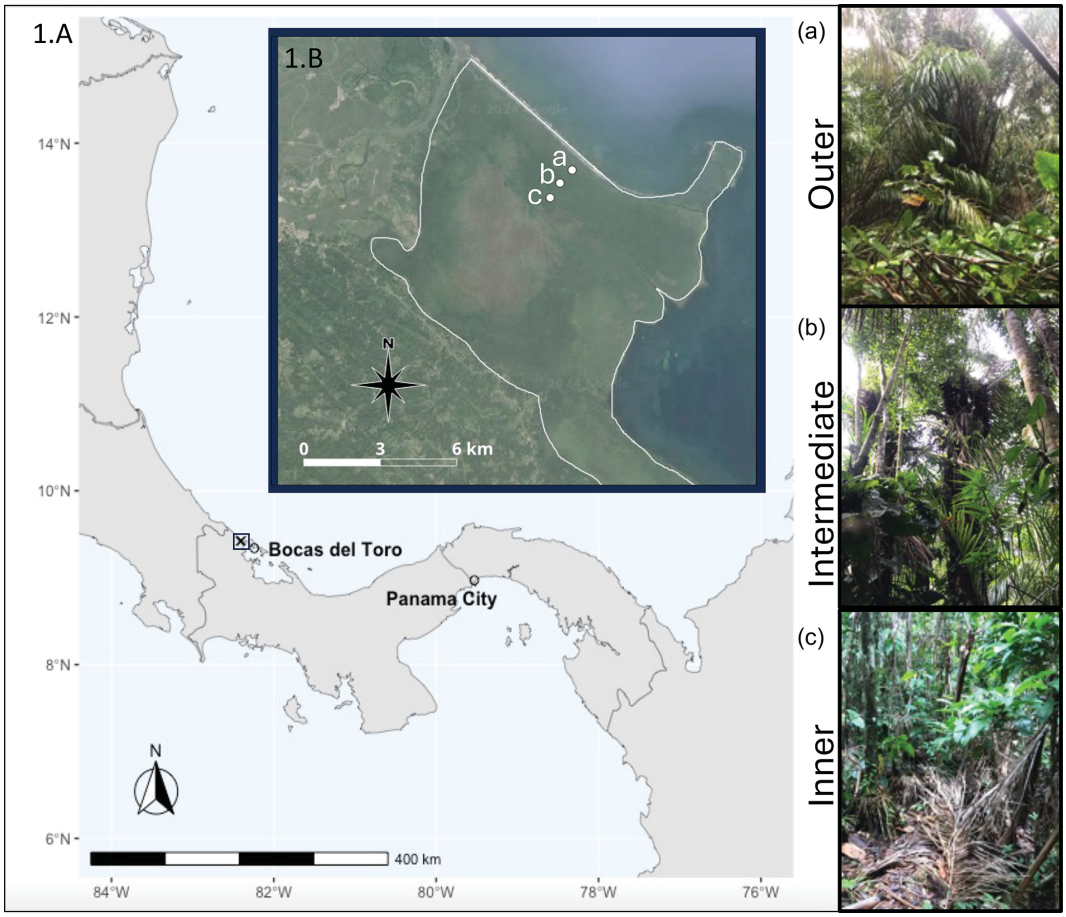

Figure 2. Map of sites included in this study from the Changuinola peat deposit. **(1.A)** Location of study site identified by the square in relation to the city of Bocas Del Toro and Panama City. **(1.B)** Inset showing the location of the sites along the transect. The sites follow a vegetation gradient with **(a)** the outer site closest to the channel, a *Raphia taedigera* palm swamp; **(b)** the intermediate site mixed forest swamp; and **(c)** the inner site closest to the centre of the peatland composed of a stunted *Campnosperma panamensis* forest swamp. The sites follow a nutrient gradient, with nutrient content decreasing from the outer site to the inner site.

2 Methods

2.1 Field site description

The Bocas del Toro Province on the Caribbean coast of Panama is home to San San-Pond Sak, which was designated a Ramsar Wetland of International Importance in 1993 (site no. 611), which highlights the global significance of this wetland. This site includes the 80 km^2 Changuinola peat deposit, an ombrotrophic domed peatland located southeast of the Changuinola River (Fig. 2). Located 10 km east from the peatland is the town of Bocas del Toro, Isla Colón, where the average annual rainfall and temperature are 4000 mm and 30 °C, respectively (Isla Colón, STRI Environmental Monitoring Station). There is continuous rainfall throughout the year with no pronounced dry season, although there are two distinct periods of lower rainfall (February–April and September–October). The water table was consistently at the surface of the peatland throughout the sampling period but has been reported to fluctuate from 20 cm above to 40 cm below the peat surface during high or low rainfall (Hoyos-Santillan et al., 2015a). Mean peat temperature 10 cm below the surface is 25 °C and shows little intra-annual variation (Wright et al., 2011). The oldest deposits in the peatland are in the centre of the dome, are estimated to have been formed 4000–4500 years ago, and are roughly 8 m deep (Phillips et al., 1997).

The Changuinola peat deposit developed from a *Raphia taedigera* palm swamp, which is unlike Southeast Asian coastal peatlands that developed from sediment-trapping mangrove stands (Anderson and Muller, 1975; Phillips et al., 1997). The vegetation communities that formed the Changuinola peat deposits have shifted spatially over time, reflecting variations in environmental conditions and resulting in spatial heterogeneities in C inputs across the peatland (Cohen et al., 1989; Phillips and Bustin, 1996). At present, there are seven distinct phasic plant communities that form concentric rings within the peat dome. From the periphery

and moving to the interior they are as follows: (i) a *Rhizophora mangle* mangrove swamp, (ii) a mixed back mangrove swamp, (iii) a *Raphia taedigera* palm swamp, (iv) a mixed forest swamp, (v) a stunted *Campnosperma panamensis* forest swamp, (vi) a sawgrass or stunted forest swamp, and (vii) a *Myrica* and *Cyrilla* bog plain (Phillips et al., 1997). Previous work showed that nutrient content in the peat was generally higher near the edge ($1200\,\mu g\,P\,g^{-1}$ and $27\,mg\,N\,g^{-1}$, where "P" is phosphorus and "N" is nitrogen) and lower in the interior of the peatland ($377\,\mu g\,P\,g^{-1}$, $22\,mg\,N\,g^{-1}$) (Sjögersten et al., 2011; Troxler, 2007, 2012).

For this study we selected sites in three of the representative plant communities with dominant vegetation and nutrient patterns that have been described previously. These include outer (*Raphia taedigera* palm swamp), intermediate (mixed forest swamp), and inner (stunted *Campnosperma panamensis* forest swamp) peatland sites (Fig. 2). Previous studies conducted within the Changuinola deposit have reported differences in peat properties, root exudate characteristics, and ex situ experimental responses in lab studies tied to the vegetation community. Previously reported surface and shallow peat (< 30 cm) CO_2 flux rates for the outer and inner sites used here varied from 320–500 $mg\,CO_2\,m^{-2}\,h^{-1}$ with no significant variation between sites (Wright et al., 2011), and subsurface peat (below 30 cm) appeared to have similar carbohydrate–aromatic C ratios at the surface (Upton et al., 2018).

2.2 Sample collection

Bulk peat, pore water samples, and greenhouse gases (CO_2 and CH_4) were collected in October 2019. We sampled from 30 cm to basal depths that were identified by a marine clay boundary at the base of the peat and did not sample surface samples (0–30 cm) that might have stronger surface vegetation influence on peat chemistry compared to deeper layers that are further along in the decomposition process (Barreto and Lindo, 2020). This study aimed to compare bulk peat and pore water components of deep peat with gas produced at the same depth, and for that reason only those deeper samples were collected. Peat cores were collected using a 5.2 cm diameter and 51 cm long peat sampler (Eijkelkamp, Product code 04.09). Bulk peat, pore water samples, and greenhouse gases (CO_2 and CH_4) were collected in October 2019 from depths of 30 ± 5 and 60 ± 5 cm, 100 ± 5, 200 ± 5, 300 ± 5, and 400 ± 5 cm depending on the total peat depth at each site. Porewater was collected using a peristaltic pump with Teflon tubing from 1.25 cm diameter PVC pipe piezometers to measure DOC from the same depths as the peat collection. Porewater was filtered with 45 µm particle retention using plastic syringes fitted with stopcocks and filters and deposited into 50 mL falcon tubes for transport. Following collection, peat cores were subsampled to coordinate with gas well depths and sealed in plastic bags to avoid oxidation during transport to the Smithsonian Tropical Research Institute soils lab in Panama City, Panama.

Diffusion gas wells were deployed at the intermediate and outer site at the same depths as pore water and peat collection to ensure robust comparison between the two source materials (bulk peat and DOC) and respiration products. There was insufficient time to include the inner site in gas collection at the time of sampling. These diffusion wells consisted of PVC pipe with mesh coverings positioned within the peat to allow water to be sampled from the desired depth without contamination of bulk peat or water pulled from other depths. Water was taken from the desired depth using a peristaltic pump and cycled into a 1 L glass container. The headspace within the glass container was allowed to equilibrate over several hours while the water was pumped through the container at a rate of 1.5–1.8 $L\,min^{-1}$. Air samples from the equilibrated headspace were taken using a syringe fitted with a stopcock and needle and deposited into evacuated 125 mL serum bottles fitted with heavy butyl rubber septa.

2.3 Elemental and isotopic analyses

The elemental composition of solid homogenized air-dried peat was analysed using an elemental analyser 205 (CHNOS) coupled to an IsoPrime 100 isotope ratio mass spectrometer at the Center for Stable Isotope Biogeochemistry (CSIB) 206 at the University of California, Berkeley. This analysis produced measurements for percent C and N, $\delta^{13}C$, and $\delta^{15}N$. The ash content of bulk peat was determined by ignition of aliquots (~ 1.0 g) at 460 °C for 5 h.

Sample preparation and analysis for $\Delta^{14}C$ was completed at the Center for Accelerator Mass Spectrometry (CAMS) at Lawrence Livermore National Laboratory. To ensure that peat samples were handled appropriately for both biogeochemistry and chronology, we measured two subsamples following homogenization with a ball and mill grinder: the first underwent acid–base–acid (ABA) pre-treatment to remove possible interfering carbonates and modern C-derived humic acids and the second received no pre-treatment (Norris et al., 2020). Samples were immersed in 1 N of hydrochloric acid (HCl) to remove carbohydrates. Humic acids were then removed from the sample with 0.25 M of sodium hydroxide (NaOH) and treated with a 1 N HCl immersion before they were rinsed with deionized water until neutral. The pre-treated samples were then placed on a heating block until dried. The two sets of peat samples had identical $\Delta^{14}C$ results and the values with no pre-treatment were used in this study (Table A1). The porewater DOC samples were acidified with 1 N HCl at 70 °C to remove dissolved inorganic C and freeze-dried. Both sets of peat samples and the residual DOC were loaded into quartz tubes with excess CuO and combusted at 900 °C to ensure complete combustion to CO_2.

Gas samples for CH_4 and CO_2 were extracted following the protocol outlined by McNicol et al. (2020). For $^{14}CO_2$ samples, a series of cryogenic traps were used to purify and

isolate the CO_2. For $^{14}CH_4$ samples, the mixed composition field samples were cryogenically purified to remove water and CO_2, and the remaining CH_4 was converted to CO_2 by combustion (Petrenko et al., 2008). Resulting CO_2 from samples was split to measure both a $\delta^{13}C$ and $\Delta^{14}C$. Extracted CO_2 and CH_4 were analysed for $\Delta^{14}C$ and $\delta^{13}C$ when possible, but some sample masses were too small for both analyses (a minimum of 20 µg C is needed for $\Delta^{14}C$ analysis, and we prioritized measurements for $\Delta^{14}C$ for the purposes of this study). The $\delta^{13}C$ values were analysed at the Stable Isotope Geosciences Facility at Texas A&M University on a Thermo Scientific MAT 253 dual-inlet stable isotope ratio mass spectrometer. To obtain a $\Delta^{14}C$ measurement, the CO_2 was reduced to graphite onto Fe powder in the presence of H_2 (Vogel et al., 1984) and analysed on the HVEC 10 MV Model FN Tandem Van de Graaff Accelerator or the NEC 1 MV Pelletron Tandem Accelerator at CAMS (Broek et al., 2021). $\Delta^{14}C$ values are reported as $\Delta^{14}C$ (‰) corrected to the year of measurement (2019) and for mass-dependent fractionation using $\delta^{13}C$ values, and age is reported in years before present (yr BP) within 2 standard deviations using the Libby half-life of 5568 years (Stuiver and Polach, 1977). Age–depth models were generated for each site in R v.4.2.2 (R Core Team, 2022) using the rbacon package v2.3.9.1. BACON (Bayesian accumulation) is based on Bayesian theory and simulates the sediment deposition process while accounting for both variable deposition rates and spatial autocorrelation of deposition from one layer to another within the core (Blaauw and Christen, 2011). Long-term peat accumulation rates were estimated by fitting linear regressions to age–depth model outputs. The calibrated ages showed the timing of peat development and accumulation between the three sites, and the conventional radiocarbon values were used to compare and identify the sources of material used to generate CO_2 and CH_4 at depth.

Differences in stable isotopic ($\delta^{13}C$) composition between $\delta^{13}CO_2$ and $\delta^{13}CH_4$ can identify the dominant pathway that produces methane because hydrogenotrophic methanogenesis fractionates against heavy C isotopes more than acetoclastic methanogenesis (Wilson et al., 2016). Based on the measured stable C isotope signatures of CH_4 ($\delta^{13}C$–CH_4) and CO_2 ($\delta^{13}C$–CO_2) in dissolved gas in peat pore water, we calculated the apparent C isotope fractionation (α_{app}) for this methanogenic process according to the following formula: $\alpha = (\delta^{13}CO_2 + 1000)/(\delta^{13}CH_4 + 1000)$. Values of $\alpha_{app} = [(\delta^{13}CO_2 + 1000)/(\delta^{13}CH_4 + 1000)]$) that are greater than 1.065 are characteristic of environments dominated by hydrogenotrophic methanogenesis, while values lower than 1.055 are characteristic of environments dominated by acetoclastic methanogenesis (Zhang et al., 2019).

2.4 The ^{13}C-NMR spectroscopy and mixing model

Solid-state ^{13}C NMR spectra of untreated peat samples were obtained at the Pacific Northwest National Laboratory in Washington state at the Environmental Molecular Science Laboratory facility using cross-polarization under magic angle spinning conditions (CP/MAS) with a Varian DirectDrive NMR spectrometer equipped with a Varian 4 mm probe. These bulk peat samples were free of charcoal. Approximately 30 mg of peat was packed in 4 mm zirconia rotors sealed with Kel-F caps. The CP spectra were acquired after 14 k scans with a MAS rate of 14 kHz, resulting in no interference from sidebands as they were outside the range of the spectrum, with a ramp–CP contact time on the proton of 1 ms and a 1 or 2 s recycle delay depending on the sample with 62.5 kHz tppm (two-pulse phase modulation) proton decoupling (Aliev, 2020). The one-dimensional 1 H NMR spectra of all samples were processed and analysed relative to the external standard adamantine. All spectra were corrected against a KBr background, and signals arising from C in the NMR probe and rotor were accounted for by subtracting the spectra of an empty rotor from the sample. Spectra were digitally processed with exponential apodization (100 Hz line broadening with the first point set to 0.50), phase correction, and baseline correction using a Bernstein polynomial fit with Mnova software (v. 14.3.3; Mestrelab Research). Peak areas were integrated within seven chemical shift regions for input to the molecular mixing model corresponding to alkyl C (0–45 ppm), N-alkyl/methoxyl C (45–60 ppm), O-alkyl C (60–95 ppm), di-O-alkyl (95–110), aromatic C (110–145 ppm), phenolic C (145–165 ppm), and carboxyl C (165–215 ppm).

We used a mixing model that incorporates six components to describe the molecular composition of samples based on ^{13}C NMR outputs (Baldock et al., 2004). This peatland soil has no visual evidence of char, meaning that the component was removed from the model. The five remaining components (carbohydrates, proteins, lipid, lignin, and carbonyl) have each been assigned a discrete percent of different regions of the ^{13}C NMR signal intensity based on our knowledge of molar elemental contents and the C content of terrestrial soil ecosystems. The measured C : N ratio of each sample was used to constrain the protein concentration of each ^{13}C NMR spectrum in the molecular mixing model. The optimization process of the molecular mixing model compares fits for all five biomolecules to models eliminating one, two, and three components. In all cases the model fit was best when all five components were included in the model (sum of squares of deviation < 6 %). The mixing model outputs are available in Table A2.

2.5 Statistics

We assessed our data at the following two scales: (1) among-site comparisons of the three sites, considering overall differences in peat characteristics and isotopic signatures, and (2) peatland-wide patterns in soil profile characteristics and relationships among peat chemistry and isotopic signatures. Relationships between peat physical properties (C and N concentrations, C : N, $\delta^{13}C$, $\delta^{15}N$, and radiocarbon) and

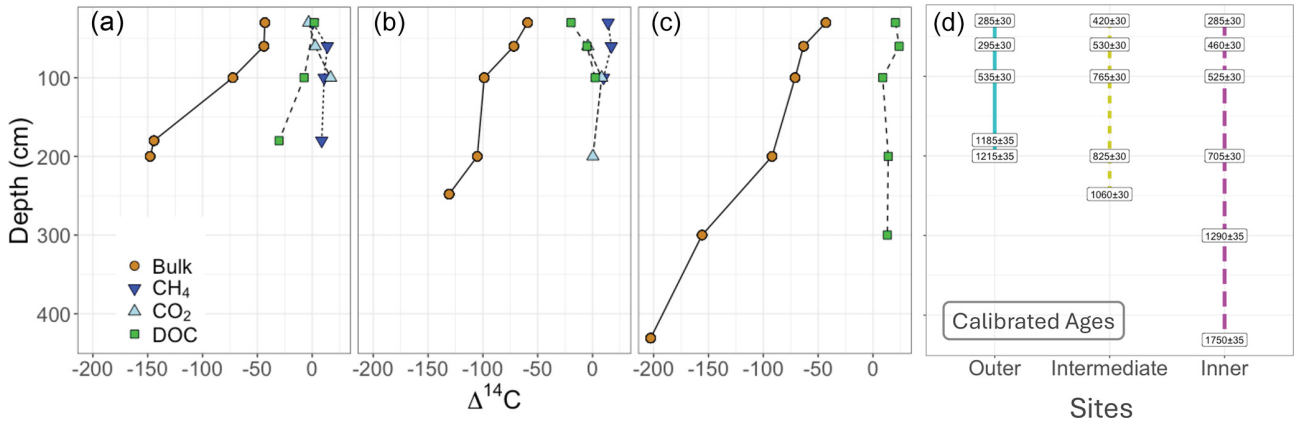

Figure 3. Isotopic composition of respiration products and substrates. Bulk peat, DOC, and respiration products (CH_4 is methane, and CO_2 is carbon dioxide) plotted by depth for the **(a)** outer, **(b)** intermediate, and **(c)** inner peatland sites. Brown circles and solid lines represent bulk peat, while green squares with dashed lines represent DOC, and these are the two measured sources for gas production. The gas products are denoted by inverted dark blue triangles and dotted lines for methane and light blue triangles and dashed lines for dissolved carbon dioxide. Note the age difference between solid peat and all DOC and gas values. This offset suggests that gas production is driven by modern DOC throughout the peat profile. **(d)** Calibrated ages for all bulk peat measured in years before present are shown within instrument error for the outer (blue), intermediate (yellow), and inner (pink) sites.

the five biomolecules identified with the molecular mixing model were assessed using Pearson correlation analysis. We also conducted separate analyses of the ^{13}C-NMR data using raw data for spectral regions. The three sites were pooled to get peatland-scale relationships between the peat physical properties and the five biomolecules versus depth. Due to the limited size of this dataset, the Spearman method was used to measure covariance, and the coefficients are reported in the full correlation matrix results, including r^2 values and significance, in Appendix A (Figs. A3 and A4). We assessed differences among the three sites using principal component analysis (PCA) based on all factors included in the correlation matrices (all peat physical properties, chemistry, and isotopes for each site). Significant trends in biomolecule abundance across depth were identified by linear regression. To identify differences between mean radiocarbon values of the sources and respiration products we utilized two-sample t tests. Bulk peat and gas products were determined by a Welch two-sample t test to account for lack of homogeneity of variance, and differences between mean radiocarbon values of DOC and gas products were assessed by Student's two-sample t test. All relationships explored were considered significant at the 0.1 alpha level. Statistical analyses were conducted in R v.4.2.2 (R Core Team, 2022). Reported means in the text are given alongside their standard error in parentheses.

3 Results

3.1 Isotopic composition of source material and respiration products

Across all sites and depths, radiocarbon signatures of dissolved CH_4 and CO_2 were relatively modern (i.e. ^{14}C-enriched) relative to peat soil and had similar Δ^{14}C values to DOC from peat pore water, indicating the dominant contribution of modern C for soil respiration and methane production (Fig. 3). Overall, the respiration products had statistically similar radiocarbon values to the DOC ($t(23) = 0.534$, $p = 0.60$) compared to the bulk peat ($t(16) = |8.67|$, $p < 0.05$) (Table A3). The radiocarbon values for the bulk peat with depth are consistent with accumulation of C over time. The calibrated basal ages for deep peat soil from the outer, intermediate, and inner sites were 1215 ± 35, 1060 ± 30, and 1750 ± 35 yr BP, respectively, indicating the age of the peatland.

3.2 Peat properties and chemistry

The percent OC across the sites ranged from 40 %–55 % from the surface to basal depths, with lower OC content and higher ash content at depth, likely reflecting the incorporation of underlying mineral sediments into base layers. The negative correlations between both OC and N concentrations with depth were not significant (Fig. 4a–c); however, the negative correlations between ash content and depth ($r(16) = -0.62$, $p \leq 0.1$) and age and depth ($r(16) = -0.93$, $p \leq 0.1$, Fig. 4) were strongly significant (Fig. A3). Bulk peat stable isotopes, δ^{13}C and δ^{15}N, showed no strong relationship with depth or site (Fig. 4d and e). Linear slopes across

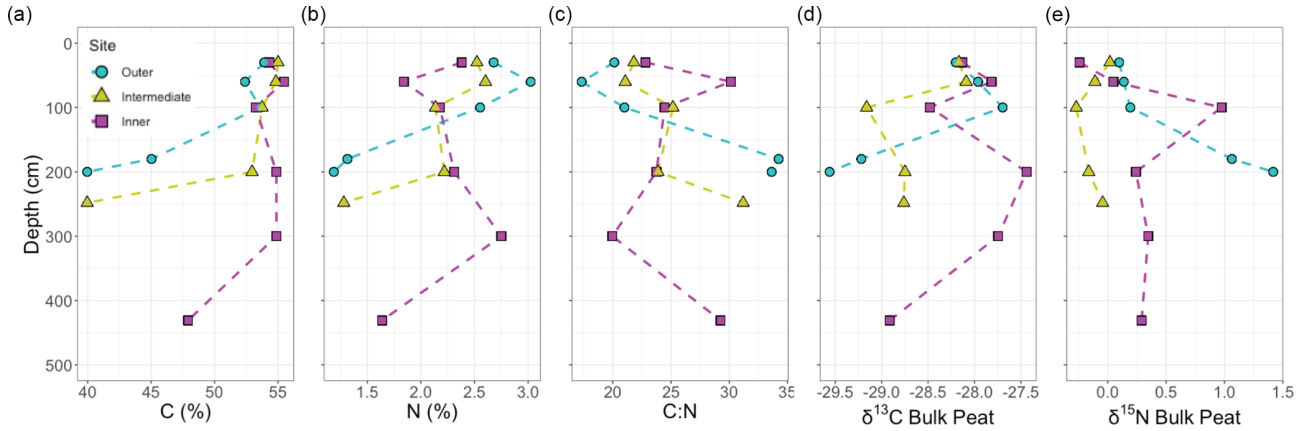

Figure 4. Bulk peat properties and characteristics. Depth profiles for **(a)** percent C, **(b)** percent N, **(c)** the ratio of C to N, **(d)** stable C isotopes, **(e)** stable N isotopes, and calibrated ages of layers measured for the three sites. Sites are indicated by colour and shape, with blue circles indicating the outer site, yellow triangles the intermediate site, and pink squares the inner site. Statistical correlations with depth were seen between ages.

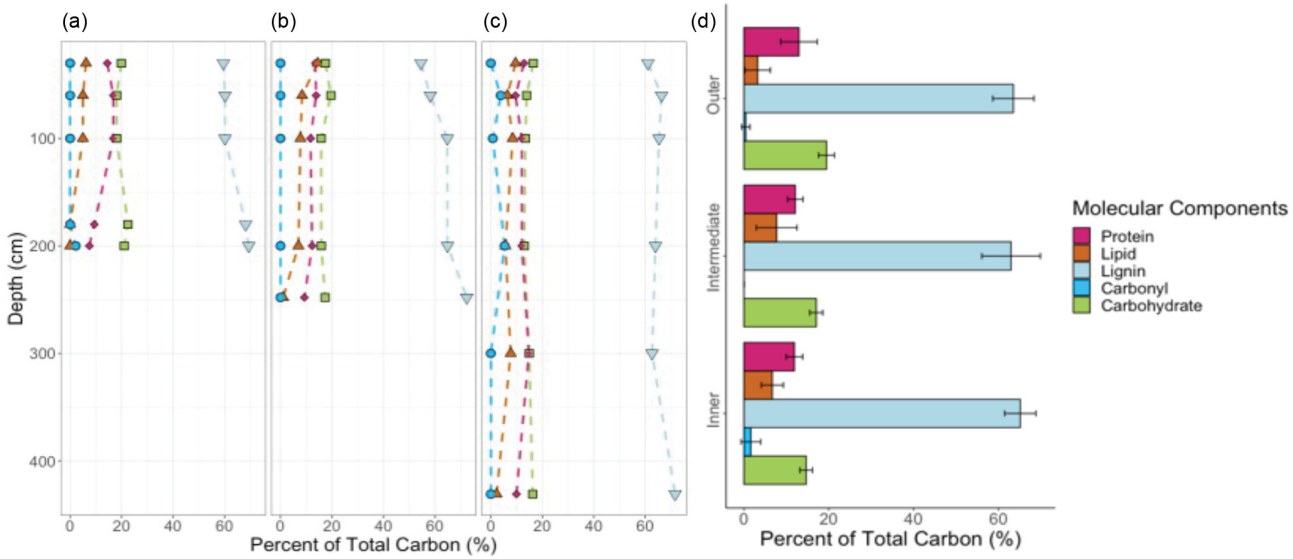

Figure 5. Proportion of total organic C attributed to each molecular component across sites and depths. Mixing model results are shown, indicating little change in the five molecular components with depth for the **(a)** outer, **(b)** intermediate, and **(c)** inner sites. Colours and symbols represent the molecular components: proteins are pink diamonds, lipids are orange triangles, lignin is shown by light blue inverted triangles, carbonyl is shown by blue circles, and carbohydrates are green squares. **(d)** Average proportions of total organic C attributed to each molecular component across sites are shown with standard error. (Note: different y axis for this figure; it does not denote depth.)

the age–depth profiles suggested consistent peat accumulation rates across the peatland over time (Fig. 4f). Estimates of long-term peat accumulation rates were calculated using the calibrated ages and were 0.192, 0.473, and 0.275 cm yr^{-1} for the outer, intermediate, and inner sites, respectively. Example spectra can be seen Fig. A1 in Appendix A. The ^{13}C-NMR molecular mixing model results showed that depth was positively correlated with lignin ($r(16) = 0.70$, $p \leq 0.1$) and negatively correlated with lipid abundance ($r(16) = -0.54$, $p \leq 0.1$) (Figs. 5a–c and A4). To further explore patterns in peat chemistry across depth, we pooled the three sites for linear regression. We found significant decreases in lipid abundance ($R^2 = 0.25$, $F(1, 14) = 5.88$, $p < 0.029$) and increases in lignin abundance ($R^2 = 0.46$, $F(1, 14) = 13.7$, $p < 0.002$) with increasing depth (Fig. A6).

Compared to the other four molecular components (protein, lipid, carbonyl, and carbohydrates), lignin was the most abundant biomarker, making up an average of 64 % ± 1.1 of peat organic matter across depths and sites (Fig. 5d). Carbohydrates were the second most abundant compound and averaged 17 % ± 0.2 across samples. There was almost no carbonyl-C present (all sites averaged < 2 %), except for in

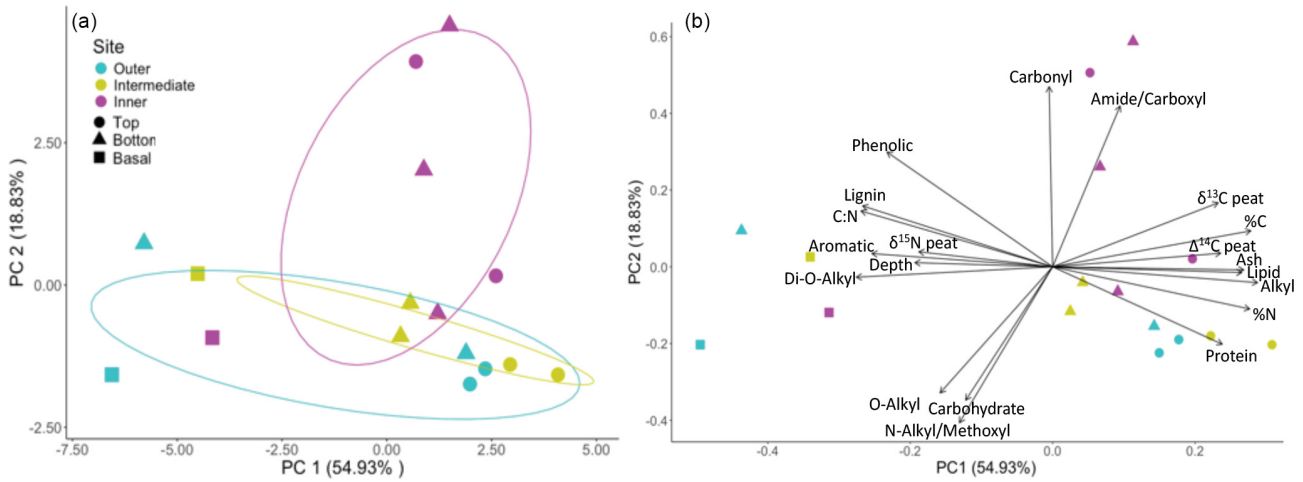

Figure 6. Clusters by site and relative factor loadings are shown here for the PCA. Panel **(a)** shows clustering by site for the outer (blue), intermediate (yellow), and inner (pink) sites, with depths indicated by shape, where the top samples (30–60 cm) are shown as circles, deep samples (> 1 m) are shown as triangles, and samples from the three basal depths (outer 200 cm, intermediate 248 cm, and inner 431 cm) are shown as squares. PC1 and PC2 samples together account for 74 % of the variance. Separation in PC1 is primarily by depth, while separation in PC2 is primarily by site **(a)**, and the factors contributing to these separations are shown in **(b)**.

deep peat at the outer site and the 60 and 200 cm layers of the inner site, which had 0.4 % ± 0.9 and 2 % ± 2 carbonyl-C, respectively (Fig. 5a and c). Overall, the organic chemistry of peat was very similar across the sites, and the main patterns that emerged were with depth.

Our PCA indicated differences in peat properties among the three sites. The scores and loadings of the first and second principal components accounted for the majority of variance (74 %), with the first principal component accounting for 54.93 % (Fig. 6a). Separation along the first principal component axis showed stratigraphic effects related to depth and peat accumulation over time, with strong separation between the 30 and 60 cm layers versus the underlying peat (shown by the symbols in Fig. 6a). The clustering of the 30 and 60 cm peat layers on PC1 can be attributed to strong axis loadings of OC, lipid, alkyl-C, and protein contributions to soil OC (Fig. 6b, Table A2). In contrast, PC2 was mainly described by site differences, with the inner site being the most distinct (Fig. 6a). This separation appeared to be tied to the loadings of carbonyl on this axis, which were different among the sites (Fig. 6b, Tables A2 and A4).

3.3 Using $\delta^{13}C$ to identify CH_4 production pathways

The α_{app} values for the methanogenesis pathway overlap between the outer and intermediate sites and averaged 1.078 (± 0.003) (Fig. 7). The data indicate no shift in α_{app} with depth throughout the peat profile. The α_{app} values indicate hydrogenotrophic methanogenesis is the dominant production pathway across all depths measured at the outer and intermediate sites.

4 Discussion

4.1 Source

The Changuinola peatland is important as an internationally protected wetland and is an example of a pristine undisturbed functioning tropical peatland. This is supported by the age–depth profiles that showed continuous undisturbed peat accumulation over the past 1060 to 1750 years. Peatland soils had similar OC and N concentrations and C : N ratios compared to other ombrotrophic peat domes across the tropics (Beilman et al., 2019; Dargie et al., 2017; Lähteenoja et al., 2012; Omar et al., 2022). Our data contribute a novel characterization of the organic components of solid and dissolved C in tropical peats and the likely contributions of these to CO_2 and CH_4 fluxes. Across all sites and depths, DOC had modern (enriched) radiocarbon signatures compared to the bulk peat, indicating it is largely derived from recent photosynthate. In contrast to the DOC originating from newer surface organic material, the solid peat becomes progressively older with depth, having accumulated over long time frames. Our data notably show an age similarity between respiration products and modern DOC radiocarbon values across depths. This strongly suggests vertical transport of modern C from the surface to deeper soil layers, which is then used in microbial metabolism. It is important to note that root exudation and turnover could also contribute modern DOC at depth, modern CO_2 values at depth could reflect root respiration, and modern root-respired CO_2 could also serve as a C source for methane production throughout the peat profile. The modern radiocarbon signature of methane at depth suggests that microbial metabolism is also dependent on modern C inputs and that older buried peat C

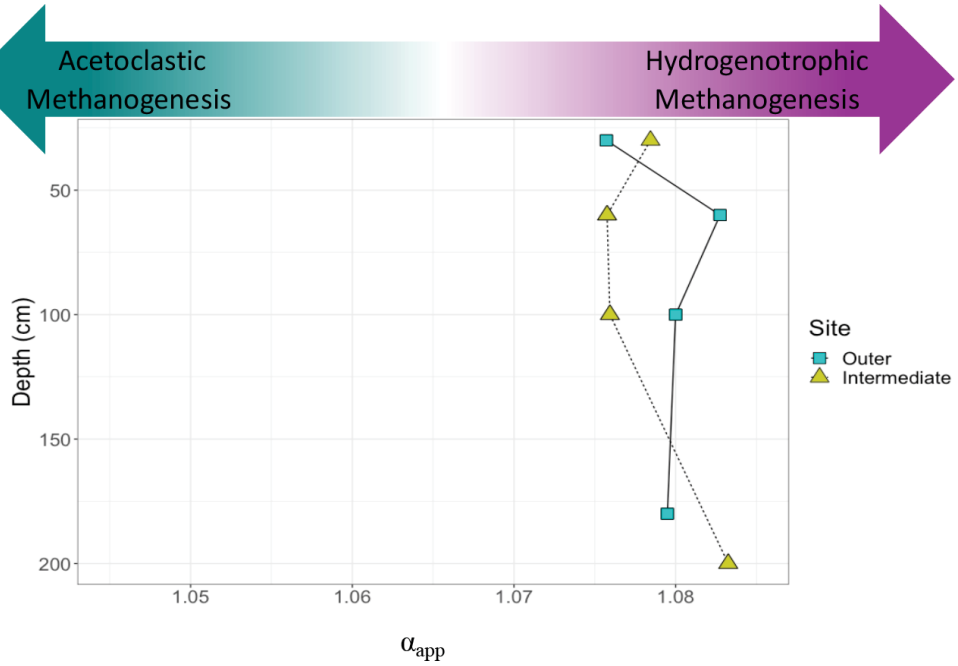

Figure 7. Differences in stable C isotopic composition between dissolved inorganic C and CH_4. Calculated estimates of the apparent fractionation factor (α_{app}) in methane production across depths are shown for gas collected from the outer (blue squares) and intermediate (green triangles) sites. The samples from the inner site did not have sufficient amounts of C for this analysis. The x axis shows little variation in α_{app} between sites and soil depths. Values of α_{app} higher than 1.065 are characteristic of environments dominated by hydrogenotrophic methanogenesis, while a value lower than 1.055 would be characteristic of acetoclastic methanogenesis (Corbett et al., 2013).

does not substantially contribute to respiration. Other tropical peatlands have showed mixed patterns of substrate age for respiration products. Similar patterns have been reported in other tropical peatlands, where modern DOC appears to be the main substrate for deep soil microbial respiration (Hoyt et al., 2020). In contrast, one peatland in Borneo reported respiration products from mixed sources (Hoyt, 2014). These contrasting results suggest that there is need to explore more tropical peatland sites to characterize substrate use by microbial metabolism in the tropics. One likely reason that deeper solid peat is not utilized as much in microbial metabolism as more modern DOC is the organic chemistry of deep peat. Specifically, deeper peat had higher lignin content than surface peat.

4.2 Peat chemistry and stabilization

The dominant biomolecule making up this peat OC was lignin, which generally represented $> 60\,\%$ of the OC in our samples. Despite the lack of a depth difference in the aromaticity index, we saw an accumulation of lignin with depth, indicating preferential preservation of this biomolecule and microbial discrimination against its decomposition through time. The waterlogged conditions in tropical peatlands can particularly reduce the decomposition of lignin by inhibiting ligninolytic microbes (Hoyos-Santillan et al., 2015b; Thormann, 2006). This selective preservation of lignin has been reported for this wetland (Hoyos-Santillan et al., 2016) and other tropical peatlands (Gandois et al., 2014) previously and supports a paradigm of selective preservation of aromatic compounds under anaerobic conditions. Coarse woody material from fallen trees, branches, and dead roots contribute a large yet relatively sporadic portion of OC inputs to tropical peat, which is in addition to the more constant inputs from leaf litter and fine root turnover (Hodgkins et al., 2018), and our data (together with the previous studies) indicate that this large-scale tree mortality and branch shedding is crucial for peat OC accumulation.

There was little change in the carbohydrate portion of peat OC with depth, although carbohydrates typically represent the most labile compounds in plant tissues for decomposition (Bader et al., 2018). This means that available carbohydrates were probably quickly decomposed at the surface, with remaining carbohydrates subsequently preserved as peat accumulated. Interestingly, there was a significant decline in lipids with depth, even though other tropical and temperate forest studies have indicated preferential preservation of lipids in upland soils (Cusack et al., 2018; Jastrow et al., 2007; Wiesenberg et al., 2010). Our data could indicate several non-exclusive patterns, including that lipids are decomposed more than other compounds under anaerobic conditions, that microbial biomass production of lipids declines,

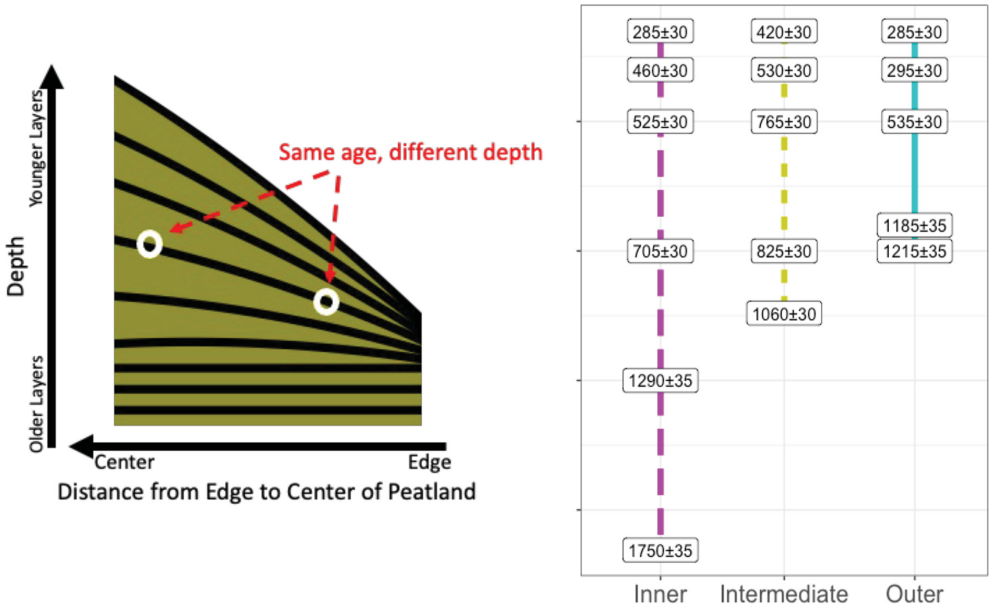

Figure 8. Schematic of peatland shape and layer accumulation pattern based on peat layer age and depth from the surface. This concept was presented in model data from Cobb et al. (2017) and has been modified to create this schematic (not to scale). Peat layers accumulate over time, with the youngest layers at the surface and the oldest layers at the base of the peat deposit. Based on this and ages collected from the sites within the Changuinola peat deposit, layers that correspond to the same age are located at different depths across the peat dome, with older peat layers being closer to the surface at the margins. Ages in the right panel are in years before present.

and/or that there were changes in the lipid content of microbial and plant C inputs to soils over time.

Surprisingly, we did not see strong differences in peatland organic chemistry among the three sites, even though plant cover did change. Our outer site is closest to the edge of the peatland in an area of the peatland that is dominated by a *Raphia taedigera* palm swamp and that has relatively high nutrient availability, whereas the intermediate site is dominated by mixed forest swamp species, and the inner site closest to the centre of the peatland is dominated by stunted *Campnosperma panamensis* forest and has relatively low nutrient availability (Phillips and Bustin, 1996; Sjögersten et al., 2011; Troxler, 2007).

Based on the $\Delta^{14}C$ age of peat collected across these sites, the dome shape of the peatland has been built up with older layers closer to the surface at the margins (Fig. 8). This shape and accumulation pattern has been described and modelled across other tropical peat domes that have the similar ombrotrophic characteristics to Changuinola (Cobb et al., 2017, 2024). Because of the organic chemistry similarities across sites, our results suggest age was not a driver of peat chemical characteristics or properties that describe decomposability. Older peat that accumulated over 1000 years ago is closer to the surface at the margins of the peatland and would thus be more vulnerable to changes in water table and aerobic conditions if there were changes in the water table or a disturbance (Dommain et al., 2011).

4.2.1 Using $\delta^{13}C$ to understand CH_4 production

In other studies from this peatland site, peat organic matter quality influences the CH_4 production pathway (Holmes et al., 2015). When easily degradable inputs are decomposed, acetate is produced by fermentative bacteria, promoting acetoclastic methanogenesis (Mobilian and Craft, 2022). After the labile material is depleted, the decomposition of more resistant material and related CO_2 production promotes hydrogenotrophic methanogenesis (Conrad, 2020). The high α_{app} (1.078 ± 0.003) values observed here indicate that hydrogenotrophic methanogenesis was the dominant production pathway across depths. CO_2 produced in the initial steps of decomposition is a strong potential supply of CO_2 to support hydrogenotrophic methanogenesis (Gruca-Rokosz and Koszelnik, 2018; Kotsyurbenko et al., 2004).

Although both northern and tropical peatlands may exhibit hydrogenotrophic methanogenesis as the dominant pathway, the $\delta^{13}C$–CH_4 signature differs widely due to variations in precursor $\delta^{13}C$–CO_2 influenced by temperature, microbial activity, organic matter composition, and decomposition processes (Holmes et al., 2015). While this study does not imply that tropical peatlands function differently from temperate peatlands, these findings suggest that research in higher-latitude peatlands offers a basis to explore OC cycling in tropical peatlands. However, additional validation is needed to confirm that they operate similarly. In summary, our findings indicate that these peatlands rely heavily on surface-

derived DOC to support microbial respiration and methanogenesis in deep peat, produce CH_4 primarily through hydrogenotrophic methanogenesis, and accumulate lignin-rich and C-dense peat at depth, with anaerobic conditions playing an important role in maintaining these processes.

4.2.2 Future implications

Tropical peatlands, such as the Changuinola peat deposit, represent critical C-rich ecosystems that play a substantial role in the global C cycle but face vulnerability under future climate scenarios. However, this C storage mechanism is sensitive to shifts in climate, hydrology, vegetation, and land use change. Changes in precipitation patterns and increased evapotranspiration associated with climate change could disrupt the connectivity between surface and deep peat layers, altering DOC transport and potentially increasing the exposure of preserved peat to aerobic conditions. The predominance of lignin, resistant under anoxic conditions, raises questions about its vulnerability when exposed to oxygen. If peatlands dry out, the preserved OC could rapidly decompose, shifting the ecosystem from a sink to a potential C source, with significant greenhouse gas release (Kettridge et al., 2015; Ofiti et al., 2023).

Our study underscores the need for further research on the resilience of tropical peatlands under changing environmental conditions. Key areas for future work include examining how shifts in vegetation and surface inputs could influence OC dynamics and gas production. Variations in plant community composition and changes in nutrient status may affect DOC quality and quantity, potentially altering the balance between acetoclastic and hydrogenotrophic methanogenesis pathways. Additionally, further investigation into the microbial communities driving peat decomposition and CH_4 production could yield insights into how these processes may shift with changing environmental factors.

Comparative studies between high-latitude and tropical peatlands highlight the unique characteristics of tropical systems, which are subject to faster biomass production and decomposition rates in warmer climates. Unlike high-latitude peatlands, which accumulate OC slowly over millennia, tropical peatlands maintain a more dynamic OC balance. This difference suggests that tropical peatlands may be particularly vulnerable to rapid changes in hydrology and land use. Understanding how such factors interact to influence peat accumulation, organic matter preservation, and greenhouse gas flux is essential for assessing the stability of tropical peatlands in a warming world.

To fully realize the climate mitigation potential of tropical peatlands, future studies must address how these ecosystems respond to both gradual and abrupt environmental changes. The development of long-term conservation and restoration strategies will depend on our ability to anticipate the impacts of altered hydrology and vegetation composition on peatland OC storage. Continued research into these processes is vital for informing global climate policies and ensuring the preservation of these irreplaceable OC reservoirs.

Appendix A

Table A1. Radiocarbon results for both untreated (no acid–base–acid, "no ABA") and treated (acid–base–acid, "ABA") sets of peat samples. Radiocarbon concentrations are expressed as $\Delta^{14}C$, and the instrument error is also given.

Site	Depth (cm)	$\Delta^{14}C$ (no ABA)	±	$\Delta^{14}C$ (ABA)	±
Outer	30	−43.1	3.4	−54.9	4.1
	60	−44.0	3.4	−54.2	4.1
	100	−72.4	3.1	−77.5	4.0
	180	−147.8	3.2	−157.6	3.6
	200	−144.3	3.2	−157.8	3.6
Intermediate	30	−59.2	3.4	−59.9	4.0
	60	−71.8	3.3	−70.2	4.0
	100	−98.8	3.3	−107.5	3.8
	200	−105.1	3.2	−110.8	3.8
	248	−130.8	3.2	−141.0	3.7
Inner	30	−42.9	3.3	−45.6	4.1
	60	−63.3	3.3	−68.5	4.0
	100	−71.0	3.2	−75.9	4.0
	200	−92.0	3.3	−93.6	3.9
	300	−155.8	3.2	−155.2	3.6
	431	−202.7	3.1	−203.1	3.4

Table A2. Mixing model outputs for all depths sampled from the three sites: the molecular component proportion of total C measured via ^{13}CNMR and described by the mixing model output as a weighted percentage (wt %), as developed by Baldock et al. (2004), and %C measured from bulk peat combustion via an elemental analyser.

Site	Depth (cm)	Molecular component	wt %	%C
Inner	30	Carbohydrate	16.5	54.33
Inner	30	Protein	12.9	54.33
Inner	30	Lignin	61.0	54.33
Inner	30	Lipid	9.6	54.33
Inner	30	Carbonyl	0.0	54.33
Inner	60	Carbohydrate	13.9	55.49
Inner	60	Protein	9.6	55.49
Inner	60	Lignin	66.3	55.49
Inner	60	Lipid	6.4	55.49
Inner	60	Carbonyl	3.8	55.49
Inner	100	Carbohydrate	13.4	53.24
Inner	100	Protein	12.1	53.24
Inner	100	Lignin	65.3	53.24
Inner	100	Lipid	8.5	53.24
Inner	100	Carbonyl	0.7	53.24
Inner	200	Carbohydrate	13.0	54.87
Inner	200	Protein	12.1	54.87
Inner	200	Lignin	64.0	54.87
Inner	200	Lipid	5.7	54.87
Inner	200	Carbonyl	5.3	54.87
Inner	300	Carbohydrate	14.9	54.88
Inner	300	Protein	14.8	54.88
Inner	300	Lignin	62.6	54.88
Inner	300	Lipid	7.7	54.88
Inner	300	Carbonyl	0.0	54.88
Inner	431	Carbohydrate	16.3	47.91
Inner	431	Protein	9.9	47.91
Inner	431	Lignin	71.6	47.91
Inner	431	Lipid	2.2	47.91
Inner	431	Carbonyl	0.0	47.91
Intermediate	30	Carbohydrate	17.4	55.01
Intermediate	30	Protein	13.5	55.01
Intermediate	30	Lignin	54.5	55.01
Intermediate	30	Lipid	14.5	55.01
Intermediate	30	Carbonyl	0.0	55.01
Intermediate	60	Carbohydrate	19.6	54.84
Intermediate	60	Protein	13.8	54.84
Intermediate	60	Lignin	58.2	54.84
Intermediate	60	Lipid	8.4	54.84
Intermediate	60	Carbonyl	0.0	54.84
Intermediate	100	Carbohydrate	15.8	53.76
Intermediate	100	Protein	11.7	53.76
Intermediate	100	Lignin	64.8	53.76
Intermediate	100	Lipid	7.7	53.76
Intermediate	100	Carbonyl	0.0	53.76
Intermediate	200	Carbohydrate	15.9	52.96
Intermediate	200	Protein	12.3	52.96
Intermediate	200	Lignin	64.9	52.96
Intermediate	200	Lipid	7.0	52.96
Intermediate	200	Carbonyl	0.0	52.96
Intermediate	248	Carbohydrate	17.3	39.96
Intermediate	248	Protein	9.3	39.96
Intermediate	248	Lignin	72.4	39.96

Table A2. Continued.

Site	Depth (cm)	Molecular component	wt %	% C
Intermediate	248	Lipid	1.0	39.96
Intermediate	248	Carbonyl	0.0	39.96
Outer	30	Carbohydrate	19.9	53.92
Outer	30	Protein	14.4	53.92
Outer	30	Lignin	59.5	53.92
Outer	30	Lipid	6.2	53.92
Outer	30	Carbonyl	0.0	53.92
Outer	60	Carbohydrate	18.1	52.40
Outer	60	Protein	16.8	52.40
Outer	60	Lignin	60.2	52.40
Outer	60	Lipid	5.0	52.40
Outer	60	Carbonyl	0.0	52.40
Outer	100	Carbohydrate	18.1	53.60
Outer	100	Protein	16.8	53.60
Outer	100	Lignin	60.2	53.60
Outer	100	Lipid	5.0	53.60
Outer	100	Carbonyl	0.0	53.60
Outer	180	Carbohydrate	22.4	39.96
Outer	180	Protein	9.4	39.96
Outer	180	Lignin	68.2	39.96
Outer	180	Lipid	0.0	39.96
Outer	180	Carbonyl	0.0	39.96
Outer	200	Carbohydrate	21.0	45.03
Outer	200	Protein	7.5	45.03
Outer	200	Lignin	69.4	45.03
Outer	200	Lipid	0.0	45.03
Outer	200	Carbonyl	2.2	45.03

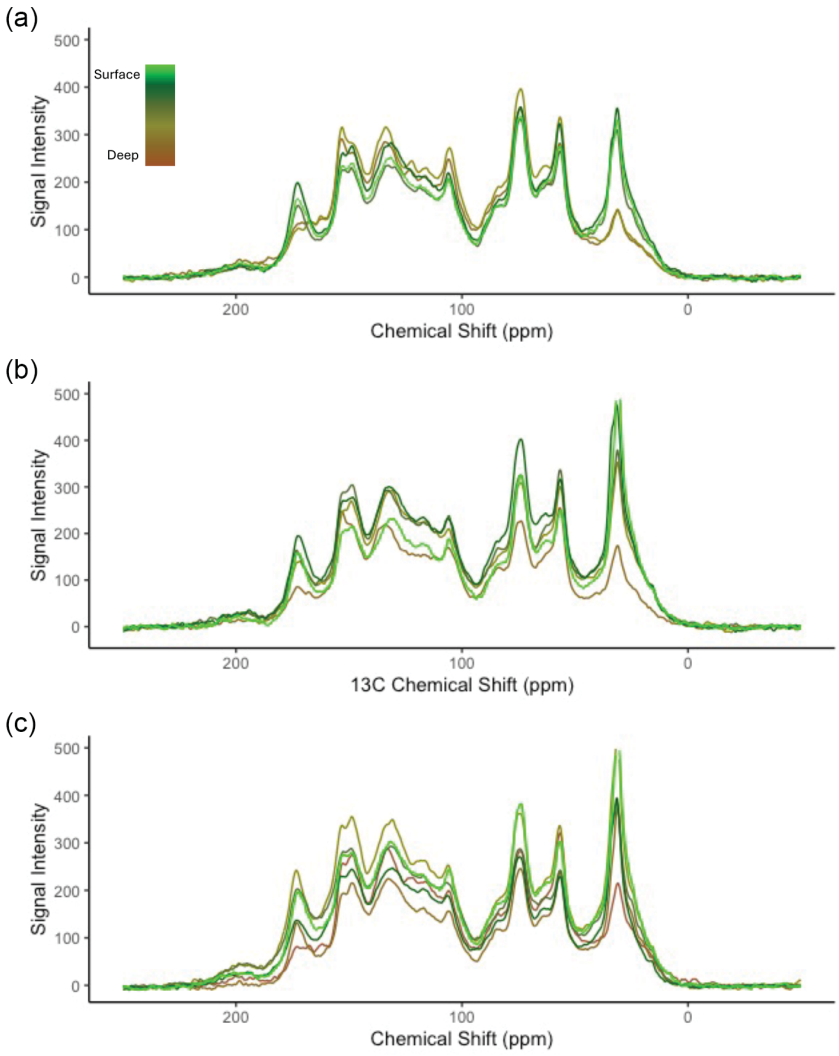

Figure A1. Stacked overlay of depth profiles of ^{13}C NMR spectra of the **(a)** outer, **(b)** intermediate, and **(c)** inner sites. Colours increase in darkness to represent an increase in depth, with light green colours representing the surface peat soil and dark browns the deeper and basal (deepest) peat soil. Peak areas were integrated corresponding to alkyl C (0–45 ppm), N-alkyl/methoxyl C (45–60 ppm), O-alkyl C (60–95 ppm), di-O-alkyl (95–110), aromatic C (110–145 ppm), phenolic C (145–165 ppm), and carboxyl C (165–215 ppm). Overall, there are very similar peak heights and areas between depths and sites, with some differences found in deep peat chemistry.

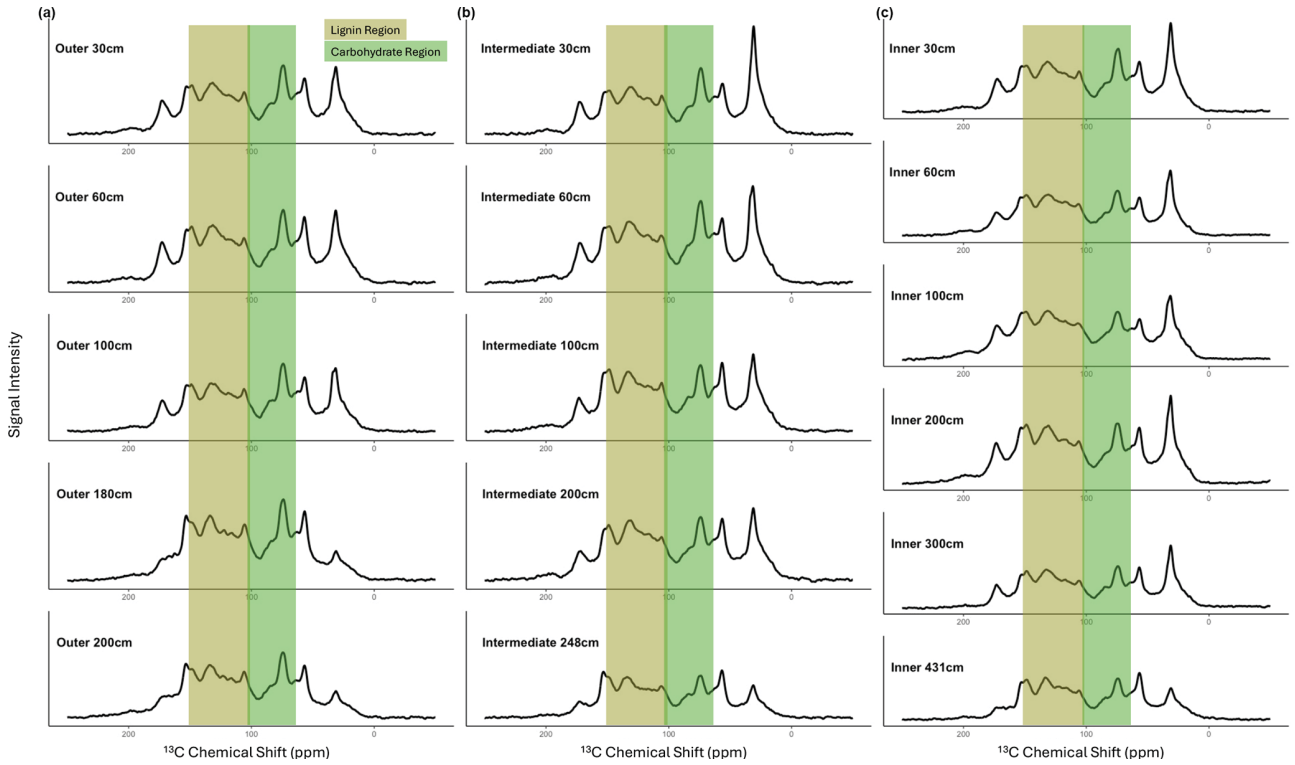

Figure A2. The ^{13}C NMR spectra of solid peat samples are shown across depth profiles for the **(a)** outer, **(b)** intermediate, and **(c)** inner peatland sites. Peak areas have been highlighted to emphasize changes in lignin (the brown range from 100–150 ppm) and carbohydrate (the green range from 60–105 ppm) across sites and depths. The *y* axis has been scaled equally across all plots to visually compare changes in peak heights and area across depths; however, the additional depth at the inner site needs to be considered when making this comparison. Overall, there are very similar peak heights and areas between depths and sites, with some differences in deep peat chemistry.

Table A3. Results from *t* tests showing bulk peat radiocarbon values versus respiration product gas radiocarbon values and DOC radiocarbon values versus respiration product gas radiocarbon values. Solid peat samples had radiocarbon values that were significantly different from the radiocarbon of gases, while soil DOC radiocarbon values were not different from those for gases. df: degrees of freedom.

	Sample type	Mean	*t* value	df	*p* value
Pair 1	Bulk peat	−96.56	−8.67	15.97	> 0.001
	Gases (CH_4, CO_2)	7.95			
Pair 2	DOC	2.03	0.54	23	0.60
	Gases (CH_4, CO_2)	−3.88			

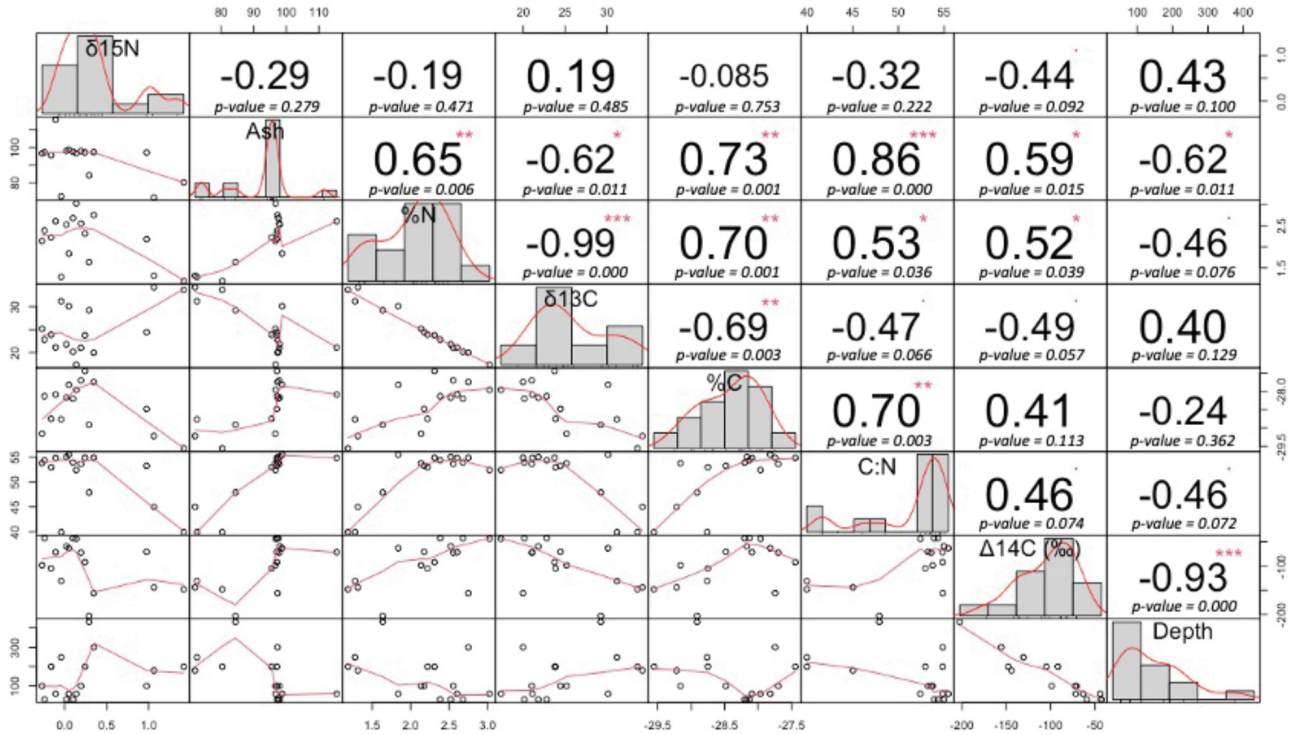

Figure A3. Correlation matrix for peat physical properties and depth. The numbers represent the value of the correlation coefficient (*r*) plus the result of the correlation test. On the bottom of the matrix are the bivariate scatterplots with a fitted line. Significance levels are > 0 ***, > 0.001**, > 0.01*, and < 0.1.

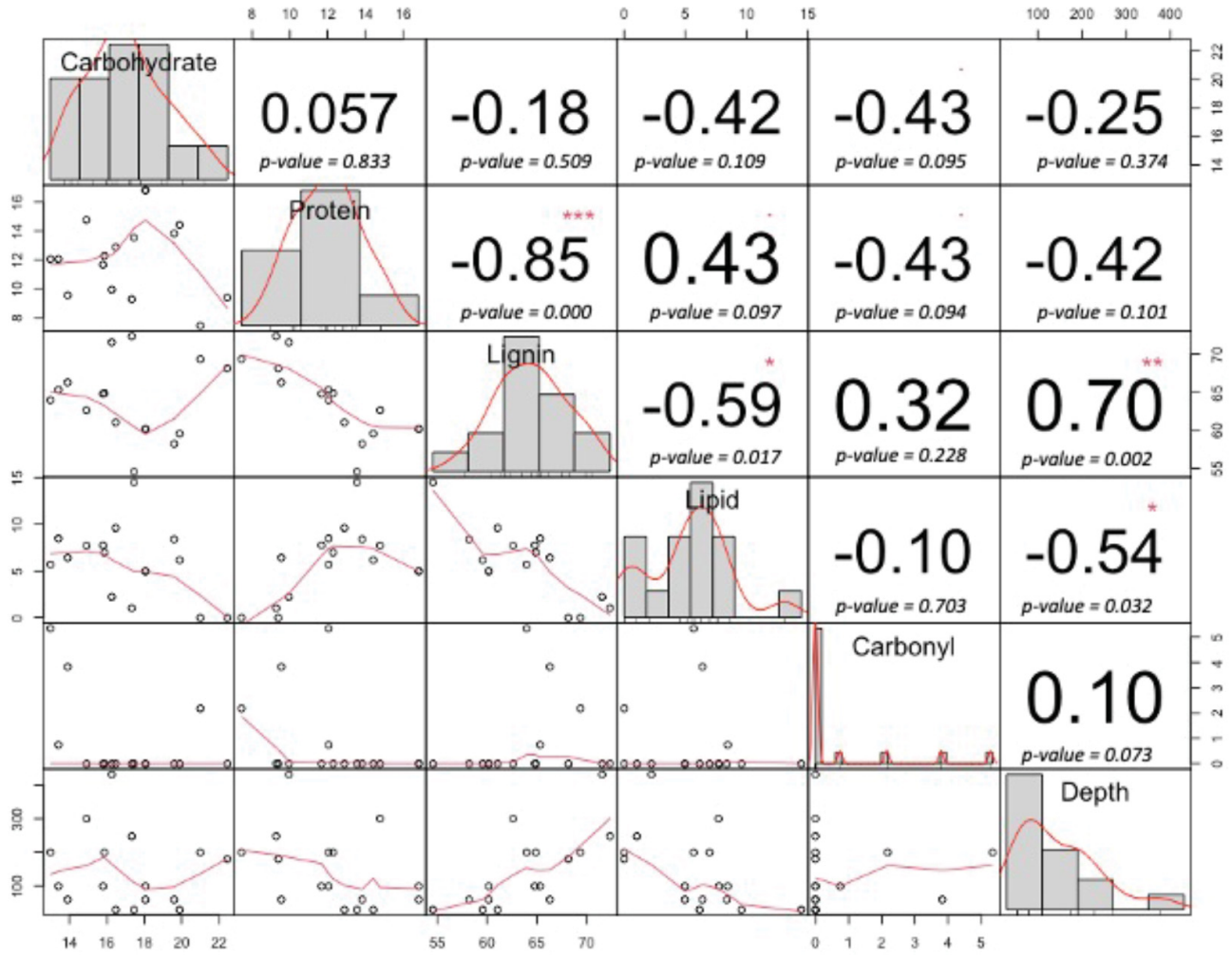

Figure A4. Correlation matrix for peat molecular components and depth. The numbers represent the value of the correlation (r^2) plus the result of the correlation test. Bivariate scatterplots with a fitted line are given at the bottom of the matrix. Significance levels are > 0 ***, > 0.001**, > 0.01*, and < 0.1.

Table A4. PCA eigenvalues and loadings for PC1 and PC2. The top positive and negative loadings on each axis have been identified in bold. LOI: loss on ignition.

	PC1	PC2
Eigenvalues	3.31	1.94
Variable		
δ^{15}N	−0.19	0.04
Ash	**−0.39**	−0.08
%N	**0.27**	−0.11
δ^{13}C	0.23	0.17
%C	0.26	0.09
C : N	**−0.27**	0.14
Δ^{14}C (‰)	0.23	0.04
Depth	−0.19	0.01
LOI	**0.27**	−0.01
Alkyl	**0.28**	−0.04
N-alkyl/methoxyl	−0.13	**−0.40**
O-alkyl	−0.16	−0.33
Di-O-alkyl	**−0.27**	−0.03
Aromatic	−0.25	0.03
Phenolic	−0.23	0.30
Amide/carboxyl	0.09	**0.41**
Carbohydrate	−0.12	**−0.34**
Protein	0.24	−0.20
Lignin	−0.26	0.16
Lipid	0.26	−0.02
Carbonyl	−0.01	**0.46**

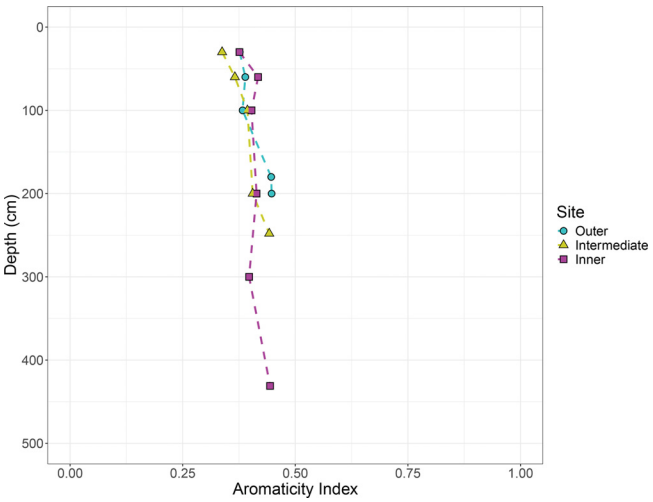

Figure A5. The aromaticity index shown here has been used to describe the decomposition state of soils. This index is expressed as the ratio of aromatic C to alkyl + O-alkyl + aromatic C and is calculated using the results from the integration of the ^{13}C NMR spectral regions. The soil is considered more decomposed as the aromaticity index approaches 1. The lack of change in aromaticity with depth and the consistency across all three sites suggest that little decomposition has occurred over space and time. Sites are indicated by colour and shape, with blue circles indicating the outer site, yellow triangles the intermediate site, and pink squares the inner site.

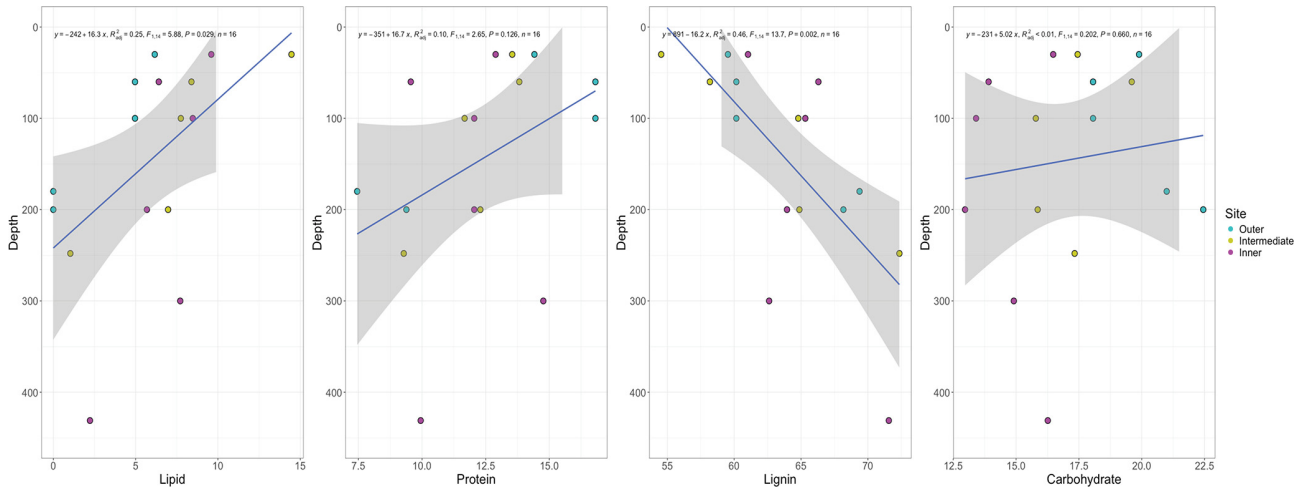

Figure A6. Linear regression of the four most abundant soil biomolecules from the mixing model versus depth. Sites have been pooled for this analysis and are indicated by colour, with blue indicating the outer site, yellow the intermediate site, and pink the inner site. Regressions show significant declines with depth for lipids and significant increases with depth for lignin across sites.

Data availability. Following publication, the data that support this paper will be publicly available at the U.S. Department of Energy's Environmental Systems Science Data Infrastructure for a Virtual Ecosystem (ESS-DIVE: https://doi.org/10.15485/2566016, Hedgpeth et al., 2025) and will be submitted to the International Soil Radiocarbon Database (https://soilradiocarbon.org/, Lawrence et al., 2020).

Author contributions. AH: conceptualization, funding acquisition, data collection, formal analysis, investigation, methodology, visualization, writing (original draft). AMH: methodology, resources, formal analysis, visualization, supervision, writing (review and editing). DFC: conceptualization, funding acquisition, methodology, supervision, visualization, writing (review and editing). KC: supervision, writing (review and editing). KJM: funding acquisition, resources, methodology, supervision, writing (review and editing). KJM and DFC should be considered joint senior authors.

Competing interests. The contact author has declared that none of the authors has any competing interests.

Disclaimer. Publisher's note: Copernicus Publications remains neutral with regard to jurisdictional claims made in the text, published maps, institutional affiliations, or any other geographical representation in this paper. While Copernicus Publications makes every effort to include appropriate place names, the final responsibility lies with the authors.

Acknowledgements. Alexandra Hedgpeth thanks the Smithsonian Tropical Research Institute for a short-term research fellowship, Eric Brown for field support, and the staff at the Smithsonian Tropical Research Institute and the Bocas del Toro field station for logistical support. This project was supported in part by a University of California-National Lab In-Residence Graduate Fellowship (no. L21GF3629) to Alexandra Hedgpeth, which was hosted by Lawrence Livermore National Laboratory. The ^{13}C-NMR analysis for this work was supported under a U.S. Department of Energy User Award (no. 60514) to Daniela F. Cusack and Alexandra Hedgpeth, which was conducted at the Environmental Molecular Sciences Laboratory. Access to field and lab sites in Panama was supported by a DOE Office of Science Early Career Award (no. DE-SC0015898) and an National Science Foundation (NSF) Geography and Spatial Studies Grant (no. BCS-1437591) to Daniela F. Cusack. We would like to thank Sarah Burton and Andrew Lipton from the Environmental Molecular Sciences Laboratory for their assistance with the ^{13}C-NMR analysis. A portion of this work was performed under the auspices of the U.S. Department of Energy by Lawrence Livermore National Laboratory (LLNL-JRNL-868401) under contract no. DE-AC52-07NA27344 and funded by a U.S. Department of Energy Office of Science Early Career Program Award (no. SCW1572) to Karis J. McFarlane. Alison M. Hoyt was supported in part by the NSF (award no. 2406964). Alexandra Hedgpeth would like to express appreciation for her dissertation committee members Glen MacDonald and Thomas Gillespie for their guidance, feedback, and support throughout the research process. We would like to thank Antonia L. Herwig, Lee Dietterich, and Makenna Brown for their assistance in the field. We acknowledge support from the Gordon and Betty Moore Foundation, Grant GBMF11519 (Advancing the understanding of methane emissions from tropical wetlands).

Financial support. This research has been supported by the University of California Research Initiatives (grant no. L21GF3629), the Environmental Molecular Sciences Laboratory (grant no. 60514), the U.S. Department of Energy (grant nos. DE-SC0015898 and

SCW1572), the National Science Foundation (grant nos. BCS-1437591, 2406964), and the Gordon and Betty Moore Foundation (grant no. GBMF11519).

Review statement. This paper was edited by Helge Niemann and reviewed by Helge Niemann and one anonymous referee.

References

Aliev, A. E.: Solid state NMR spectroscopy, in: Nuclear Magnetic Resonance, edited by: Hodgkinson, P., The Royal Society of Chemistry, 139–187, https://doi.org/10.1039/9781788010665-00139, 2020.

Anderson, J. A. R. and Muller, J.: Palynological study of a holocene peat and a miocene coal deposit from NW Borneo, Rev. Palaeobot. Palyno., 19, 291–351, https://doi.org/10.1016/0034-6667(75)90049-4, 1975.

Aravena, R., Warner, B. G., Charman, D. J., Belyea, L. R., Mathur, S. P., and Dinel, H.: Carbon Isotopic Composition of Deep Carbon Gases in an Ombrogenous Peatland, Northwestern Ontario, Canada, Radiocarbon, 35, 271–276, https://doi.org/10.1017/S0033822200064948, 1993.

Bader, C., Müller, M., Schulin, R., and Leifeld, J.: Peat decomposability in managed organic soils in relation to land use, organic matter composition and temperature, Biogeosciences, 15, 703–719, https://doi.org/10.5194/bg-15-703-2018, 2018.

Baldock, J. A., Masiello, C. A., Gélinas, Y., and Hedges, J. I.: Cycling and composition of organic matter in terrestrial and marine ecosystems, Mar. Chem., 92, 39–64, https://doi.org/10.1016/j.marchem.2004.06.016, 2004.

Barkhordarian, A., Saatchi, S. S., Behrangi, A., Loikith, P. C., and Mechoso, C. R.: A Recent Systematic Increase in Vapor Pressure Deficit over Tropical South America, Sci. Rep., 9, 15331, https://doi.org/10.1038/s41598-019-51857-8, 2019.

Barreto, C. and Lindo, Z.: Decomposition in Peatlands: Who Are the Players and What Affects Them?, Front. Young Minds, 8, 107, https://doi.org/10.3389/frym.2020.00107, 2020.

Barros, V. R., Field, C. B., Dokken, D. J., Mastrandrea, M. D., and Mach, K. J. (Eds.): Central and South America, in: Climate Change 2014: Impacts, Adaptation and Vulnerability, Cambridge University Press, Cambridge, 1499–1566, https://doi.org/10.1017/CBO9781107415386.007, 2014.

Beilman, D. W., Massa, C., Nichols, J. E., Elison Timm, O., Kallstrom, R., and Dunbar-Co, S.: Dynamic Holocene Vegetation and North Pacific Hydroclimate Recorded in a Mountain Peatland, Moloka'i, Hawai'i, Front. Earth Sci., 7, 188, https://doi.org/10.3389/feart.2019.00188, 2019.

Blaauw, M. and Christen, J. A.: Flexible paleoclimate age-depth models using an autoregressive gamma process, Bayesian Anal., 6, 457–474, https://doi.org/10.1214/11-BA618, 2011.

Broek, T. A. B., Ognibene, T. J., McFarlane, K. J., Moreland, K. C., Brown, T. A., and Bench, G.: Conversion of the LLNL/-CAMS 1 MV biomedical AMS system to a semi-automated natural abundance ^{14}C spectrometer: system optimization and performance evaluation, Nucl. Instrum. Meth. B, 499, 124–132, https://doi.org/10.1016/j.nimb.2021.01.022, 2021.

Chadwick, R., Good, P., Martin, G., and Rowell, D. P.: Large rainfall changes consistently projected over substantial areas of tropical land, Nat. Clim. Change, 6, 177–181, https://doi.org/10.1038/nclimate2805, 2016.

Chanton, J. P., Bauer, J. E., Glaser, P. A., Siegel, D. I., Kelley, C. A., Tyler, S. C., Romanowicz, E. H., and Lazrus, A.: Radiocarbon evidence for the substrates supporting methane formation within northern Minnesota peatlands, Geochim. Cosmochim. Ac., 59, 3663–3668, https://doi.org/10.1016/0016-7037(95)00240-Z, 1995.

Chanton, J. P., Glaser, P. H., Chasar, L. S., Burdige, D. J., Hines, M. E., Siegel, D. I., Tremblay, L. B., and Cooper, W. T.: Radiocarbon evidence for the importance of surface vegetation on fermentation and methanogenesis in contrasting types of boreal peatlands, Global Biogeochem. Cy., 22, 2008GB003274, https://doi.org/10.1029/2008GB003274, 2008.

Clymo, R. S., Turunen, J., and Tolonen, K.: Carbon Accumulation in Peatland, Oikos, 81, 368, https://doi.org/10.2307/3547057, 1998.

Cobb, A. R., Hoyt, A. M., Gandois, L., Eri, J., Dommain, R., Abu Salim, K., Kai, F. M., Haji Su'ut, N. S., and Harvey, C. F.: How temporal patterns in rainfall determine the geomorphology and carbon fluxes of tropical peatlands, P. Natl. Acad. Sci. USA, 114, https://doi.org/10.1073/pnas.1701090114, 2017.

Cobb, A. R., Dommain, R., Yeap, K., Hannan, C., Dadap, N. C., Bookhagen, B., Glaser, P. H., and Harvey, C. F.: A unified explanation for the morphology of raised peatlands, Nature, 625, 79–84, https://doi.org/10.1038/s41586-023-06807-w, 2024.

Cohen, A. D., Raymond, R., Ramirez, A., Morales, Z., and Ponce, F.: The Changuinola peat deposit of northwestern Panama: a tropical, back-barrier, peat(coal)-forming environment, Int. J. Coal Geol., 12, 157–192, https://doi.org/10.1016/0166-5162(89)90050-5, 1989.

Conrad, R.: Importance of hydrogenotrophic, aceticlastic and methylotrophic methanogenesis for methane production in terrestrial, aquatic and other anoxic environments: A mini review, Pedosphere, 30, 25–39, https://doi.org/10.1016/S1002-0160(18)60052-9, 2020.

Corbett, J. E., Tfaily, M. M., Burdige, D. J., Cooper, W. T., Glaser, P. H., and Chanton, J. P.: Partitioning pathways of CO_2 production in peatlands with stable carbon isotopes, Biogeochemistry, 114, 327–340, https://doi.org/10.1007/s10533-012-9813-1, 2013.

Cusack, D. F., Markesteijn, L., Condit, R., Lewis, O. T., and Turner, B. L.: Soil carbon stocks across tropical forests of Panama regulated by base cation effects on fine roots, Biogeochemistry, 137, 253–266, https://doi.org/10.1007/s10533-017-0416-8, 2018.

Dargie, G. C., Lewis, S. L., Lawson, I. T., Mitchard, E. T. A., Page, S. E., Bocko, Y. E., and Ifo, S. A.: Age, extent and carbon storage of the central Congo Basin peatland complex, Nature, 542, 86–90, https://doi.org/10.1038/nature21048, 2017.

Dhandapani, S., Girkin, N. T., and Evers, S.: Spatial variability of surface peat properties and carbon emissions in a tropical peatland oil palm monoculture during a dry season, Soil Use Manage., 38, 381–395, https://doi.org/10.1111/sum.12741, 2022.

Dhandapani, S., Evers, S., Boyd, D., Evans, C. D., Page, S., Parish, F., and Sjogersten, S.: Assessment of differences in peat physicochemical properties, surface subsidence and GHG emissions between the major land-uses of Selangor peatlands, CATENA, 230, 107255, https://doi.org/10.1016/j.catena.2023.107255, 2023.

Dommain, R., Couwenberg, J., and Joosten, H.: Development and carbon sequestration of tropical peat domes in south-east Asia: links to post-glacial sea-level changes and Holocene climate variability, Quaternary Sci. Rev., 30, 999–1010, https://doi.org/10.1016/j.quascirev.2011.01.018, 2011.

Dommain, R., Cobb, A. R., Joosten, H., Glaser, P. H., Chua, A. F. L., Gandois, L., Kai, F., Noren, A., Salim, K. A., Su'ut, N. S. H., and Harvey, C. F.: Forest dynamics and tip-up pools drive pulses of high carbon accumulation rates in a tropical peat dome in Borneo (Southeast Asia), J. Geophys. Res.-Biogeo., 120, 617–640, https://doi.org/10.1002/2014JG002796, 2015.

Duffy, K., Gouhier, T. C., and Ganguly, A. R.: Climate-mediated shifts in temperature fluctuations promote extinction risk, Nat. Clim. Change, 12, 1037–1044, https://doi.org/10.1038/s41558-022-01490-7, 2022.

Farmer, J., Matthews, R., Smith, J. U., Smith, P., and Singh, B. K.: Assessing existing peatland models for their applicability for modelling greenhouse gas emissions from tropical peat soils, Curr. Opin. Env. Sust., 3, 339–349, https://doi.org/10.1016/j.cosust.2011.08.010, 2011.

Feng, S. and Fu, Q.: Expansion of global drylands under a warming climate, Atmos. Chem. Phys., 13, 10081–10094, https://doi.org/10.5194/acp-13-10081-2013, 2013.

Fritts, R.: Tropical Wetlands Emit More Methane Than Previously Thought, Eos, 103, https://doi.org/10.1029/2022EO220443, 2022.

Gandois, L., Teisserenc, R., Cobb, A. R., Chieng, H. I., Lim, L. B. L., Kamariah, A. S., Hoyt, A., and Harvey, C. F.: Origin, composition, and transformation of dissolved organic matter in tropical peatlands, Geochim. Cosmochim. Ac., 137, 35–47, https://doi.org/10.1016/j.gca.2014.03.012, 2014.

Girkin, N. T., Turner, B. L., Ostle, N., Craigon, J., and Sjögersten, S.: Root exudate analogues accelerate CO_2 and CH_4 production in tropical peat, Soil Biol. Biochem., 117, 48–55, https://doi.org/10.1016/j.soilbio.2017.11.008, 2018.

Girkin, N. T., Vane, C. H., Cooper, H. V., Moss-Hayes, V., Craigon, J., Turner, B. L., Ostle, N., and Sjögersten, S.: Spatial variability of organic matter properties determines methane fluxes in a tropical forested peatland, Biogeochemistry, 142, 231–245, https://doi.org/10.1007/s10533-018-0531-1, 2019.

Girkin, N. T., Dhandapani, S., Evers, S., Ostle, N., Turner, B. L., and Sjögersten, S.: Interactions between labile carbon, temperature and land use regulate carbon dioxide and methane production in tropical peat, Biogeochemistry, 147, 87–97, https://doi.org/10.1007/s10533-019-00632-y, 2020.

Girkin, N. T., Cooper, H. V., Ledger, M. J., O'Reilly, P., Thornton, S. A., Åkesson, C. M., Cole, L. E. S., Hapsari, K. A., Hawthorne, D., and Roucoux, K. H.: Tropical peatlands in the Anthropocene: The present and the future, Anthropocene, 40, 100354, https://doi.org/10.1016/j.ancene.2022.100354, 2022.

Goldstein, A., Turner, W. R., Spawn, S. A., Anderson-Teixeira, K. J., Cook-Patton, S., Fargione, J., Gibbs, H. K., Griscom, B., Hewson, J. H., Howard, J. F., Ledezma, J. C., Page, S., Koh, L. P., Rockström, J., Sanderman, J., and Hole, D. G.: Protecting irrecoverable carbon in Earth's ecosystems, Nat. Clim. Change, 10, 287–295, https://doi.org/10.1038/s41558-020-0738-8, 2020.

Gruca-Rokosz, R. and Koszelnik, P.: Production pathways for CH_4 and CO_2 in sediments of two freshwater ecosystems in south-eastern Poland, PLOS ONE, 13, e0199755, https://doi.org/10.1371/journal.pone.0199755, 2018.

Hedgpeth, A., Hoyt, A., Cavanaugh, K., McFarlane, K., and Cusack, D.: Changuinola peat soil characteristics and gas emission raw data October 2019, ESS-DIVE repository [data set], https://doi.org/10.15485/2566016, 2025.

Hirano, T., Jauhiainen, J., Inoue, T., and Takahashi, H.: Controls on the Carbon Balance of Tropical Peatlands, Ecosystems, 12, 873–887, https://doi.org/10.1007/s10021-008-9209-1, 2009.

Hodgkins, S. B., Richardson, C. J., Dommain, R., Wang, H., Glaser, P. H., Verbeke, B., Winkler, B. R., Cobb, A. R., Rich, V. I., Missilmani, M., Flanagan, N., Ho, M., Hoyt, A. M., Harvey, C. F., Vining, S. R., Hough, M. A., Moore, T. R., Richard, P. J. H., De La Cruz, F. B., Toufaily, J., Hamdan, R., Cooper, W. T., and Chanton, J. P.: Tropical peatland carbon storage linked to global latitudinal trends in peat recalcitrance, Nat. Commun., 9, 3640, https://doi.org/10.1038/s41467-018-06050-2, 2018.

Holmes, M. E., Chanton, J. P., Tfaily, M. M., and Ogram, A.: CO_2 and CH_4 isotope compositions and production pathways in a tropical peatland, Global Biogeochem. Cy., 29, 1–18, https://doi.org/10.1002/2014GB004951, 2015.

Hornibrook, E. R. C., Longstaffe, F. J., and Fyfe, W. S.: Evolution of stable carbon isotope compositions for methane and carbon dioxide in freshwater wetlands and other anaerobic environments, Geochim. Cosmochim. Ac., 64, 1013–1027, https://doi.org/10.1016/S0016-7037(99)00321-X, 2000.

Hoyos-Santillan, J., Lomax, B. H., Large, D., Turner, B. L., Boom, A., Lopez, O. R., and Sjo¨gersten, S.: Getting to the root of the problem: litter decomposition and peat formation in lowland Neotropical peatlands, Biogeochemistry, 126, 115–129, https://doi.org/10.1007/s10533-015-0147-7, 2015a.

Hoyos-Santillan, J., Lomax, B. H., Large, D., Turner, B. L., Boom, A., Lopez, O. R., and Sjögersten, S.: Getting to the root of the problem: litter decomposition and peat formation in lowland Neotropical peatlands, Biogeochemistry, 126, 115–129, https://doi.org/10.1007/s10533-015-0147-7, 2015b.

Hoyos-Santillan, J., Lomax, B. H., Large, D., Turner, B. L., Boom, A., Lopez, O. R., and Sjögersten, S.: Quality not quantity: Organic matter composition controls of CO_2 and CH_4 fluxes in neotropical peat profiles, Soil Biol. Biochem., 103, 86–96, https://doi.org/10.1016/j.soilbio.2016.08.017, 2016.

Hoyos-Santillan, J., Lomax, B. H., Large, D., Turner, B. L., Lopez, O. R., Boom, A., Sepulveda-Jauregui, A., and Sjögersten, S.: Evaluation of vegetation communities, water table, and peat composition as drivers of greenhouse gas emissions in lowland tropical peatlands, Sci. Total Environ., 688, 1193–1204, https://doi.org/10.1016/j.scitotenv.2019.06.366, 2019.

Hoyt, A.: Methane production and transport in a tropical peatland, AGU Fall Meeting Abstracts, AGU Fall Meeting Abstracts, San Francisco, California, 15–19 December 2014, B24C-06, 2014.

Hoyt, A., Cadillo-Quiroz, H., Xu, X., Torn, M., Bazán Pacaya, A., Jacobs, M., Shapiama Peña, R., Ramirez Navarro, D., Urquiza-Muñoz, D., and Trumbore, S.: Isotopic Insights into Methane Production and Emission in Diverse Amazonian Peatlands, oral, https://doi.org/10.5194/egusphere-egu2020-12960, 2020.

Hoyt, A. M., Gandois, L., Eri, J., Kai, F. M., Harvey, C. F., and Cobb, A. R.: CO_2 emissions from an undrained tropical peatland: Interacting influences of temperature, shading

and water table depth, Glob. Change Biol., 25, 2885–2899, https://doi.org/10.1111/gcb.14702, 2019.

Ingram, H. A. P.: Ecohydrology of Scottish peatlands, T. Roy. Soc. Edin.-Earth, 78, 287–296, https://doi.org/10.1017/S0263593300011226, 1987.

Jastrow, J. D., Amonette, J. E., and Bailey, V. L.: Mechanisms controlling soil carbon turnover and their potential application for enhancing carbon sequestration, Climatic Change, 80, 5–23, https://doi.org/10.1007/s10584-006-9178-3, 2007.

Jauhiainen, J., Takahashi, H., Heikkinen, J. E. P., Martikainen, P. J., and Vasander, H.: Carbon fluxes from a tropical peat swamp forest floor, Glob. Change Biol., 11, 1788–1797, https://doi.org/10.1111/j.1365-2486.2005.001031.x, 2005.

Jauhiainen, J., Kerojoki, O., Silvennoinen, H., Limin, S., and Vasander, H.: Heterotrophic respiration in drained tropical peat is greatly affected by temperature—a passive ecosystem cooling experiment, Environ. Res. Lett., 9, 105013, https://doi.org/10.1088/1748-9326/9/10/105013, 2014.

Kettridge, N., Turetsky, M. R., Sherwood, J. H., Thompson, D. K., Miller, C. A., Benscoter, B. W., Flannigan, M. D., Wotton, B. M., and Waddington, J. M.: Moderate drop in water table increases peatland vulnerability to post-fire regime shift, Sci. Rep., 5, 8063, https://doi.org/10.1038/srep08063, 2015.

Kotsyurbenko, O. R., Chin, K.-J., Glagolev, M. V., Stubner, S., Simankova, M. V., Nozhevnikova, A. N., and Conrad, R.: Acetoclastic and hydrogenotrophic methane production and methanogenic populations in an acidic West-Siberian peat bog, Environ. Microbiol., 6, 1159–1173, https://doi.org/10.1111/j.1462-2920.2004.00634.x, 2004.

Lähteenoja, O., Reátegui, Y. R., Räsänen, M., Torres, D. D. C., Oinonen, M., and Page, S.: The large Amazonian peatland carbon sink in the subsiding Pastaza-Marañón foreland basin, Peru, Glob. Change Biol., 18, 164–178, https://doi.org/10.1111/j.1365-2486.2011.02504.x, 2012.

Lampela, M., Jauhiainen, J., and Vasander, H.: Surface peat structure and chemistry in a tropical peat swamp forest, Plant Soil, 382, 329–347, https://doi.org/10.1007/s11104-014-2187-5, 2014.

Lawrence, C. R., Beem-Miller, J., Hoyt, A. M., Monroe, G., Sierra, C. A., Stoner, S., Heckman, K., Blankinship, J. C., Crow, S. E., McNicol, G., Trumbore, S., Levine, P. A., Vindušková, O., Todd-Brown, K., Rasmussen, C., Hicks Pries, C. E., Schädel, C., McFarlane, K., Doetterl, S., Hatté, C., He, Y., Treat, C., Harden, J. W., Torn, M. S., Estop-Aragonés, C., Asefaw Berhe, A., Keiluweit, M., Della Rosa Kuhnen, Á., Marin-Spiotta, E., Plante, A. F., Thompson, A., Shi, Z., Schimel, J. P., Vaughn, L. J. S., von Fromm, S. F., and Wagai, R.: An open-source database for the synthesis of soil radiocarbon data: International Soil Radiocarbon Database (ISRaD) version 1.0, Earth Syst. Sci. Data, 12, 61–76, https://doi.org/10.5194/essd-12-61-2020, 2020 (data available at: https://soilradiocarbon.org/, last access: January 2024).

Liebner, S., Ganzert, L., Kiss, A., Yang, S., Wagner, D., and Svenning, M. M.: Shifts in methanogenic community composition and methane fluxes along the degradation of discontinuous permafrost, Front. Microbiol., 6, 1–10, https://doi.org/10.3389/fmicb.2015.00356, 2015.

Loisel, J., Gallego-Sala, A. V., Amesbury, M. J., Magnan, G., Anshari, G., Beilman, D. W., Benavides, J. C., Blewett, J., Camill, P., Charman, D. J., Chawchai, S., Hedgpeth, A., Kleinen, T., Korhola, A., Large, D., Mansilla, C. A., Müller, J., Van Bellen, S., West, J. B., Yu, Z., Bubier, J. L., Garneau, M., Moore, T., Sannel, A. B. K., Page, S., Väliranta, M., Bechtold, M., Brovkin, V., Cole, L. E. S., Chanton, J. P., Christensen, T. R., Davies, M. A., De Vleeschouwer, F., Finkelstein, S. A., Frolking, S., Gałka, M., Gandois, L., Girkin, N., Harris, L. I., Heinemeyer, A., Hoyt, A. M., Jones, M. C., Joos, F., Juutinen, S., Kaiser, K., Lacourse, T., Lamentowicz, M., Larmola, T., Leifeld, J., Lohila, A., Milner, A. M., Minkkinen, K., Moss, P., Naafs, B. D. A., Nichols, J., O'Donnell, J., Payne, R., Philben, M., Piilo, S., Quillet, A., Ratnayake, A. S., Roland, T. P., Sjögersten, S., Sonnentag, O., Swindles, G. T., Swinnen, W., Talbot, J., Treat, C., Valach, A. C., and Wu, J.: Expert assessment of future vulnerability of the global peatland carbon sink, Nat. Clim. Change, 11, 70–77, https://doi.org/10.1038/s41558-020-00944-0, 2021.

McNicol, G., Knox, S. H., Guilderson, T. P., Baldocchi, D. D., and Silver, W. L.: Where old meets new: An ecosystem study of methanogenesis in a reflooded agricultural peatland, Glob. Change Biol., 26, 772–785, https://doi.org/10.1111/gcb.14916, 2020.

Mobilian, C. and Craft, C. B.: Wetland Soils: Physical and Chemical Properties and Biogeochemical Processes, in: Encyclopedia of Inland Waters, edited by: Mehner, T. and Tockner, K., Elsevier, Second edition, https://doi.org/10.1016/B978-0-12-819166-8.00049-9, 157–168, 2022.

Moore, S., Evans, C. D., Page, S. E., Garnett, M. H., Jones, T. G., Freeman, C., Hooijer, A., Wiltshire, A. J., Limin, S. H., and Gauci, V.: Deep instability of deforested tropical peatlands revealed by fluvial organic carbon fluxes, Nature, 493, 660–663, https://doi.org/10.1038/nature11818, 2013.

Noon, M. L., Goldstein, A., Ledezma, J. C., Roehrdanz, P. R., Cook-Patton, S. C., Spawn-Lee, S. A., Wright, T. M., Gonzalez-Roglich, M., Hole, D. G., Rockström, J., and Turner, W. R.: Mapping the irrecoverable carbon in Earth's ecosystems, Nat. Sustain., 5, 37–46, https://doi.org/10.1038/s41893-021-00803-6, 2021.

Norris, M. W., Turnbull, J. C., Howarth, J. D., and Vandergoes, M. J.: Pretreatment of Terrestrial Macrofossils, Radiocarbon, 62, 349–360, https://doi.org/10.1017/RDC.2020.8, 2020.

Nottingham, A. T., Bååth, E., Reischke, S., Salinas, N., and Meir, P.: Adaptation of soil microbial growth to temperature: Using a tropical elevation gradient to predict future changes, Glob. Change Biol., 25, 827–838, https://doi.org/10.1111/gcb.14502, 2019.

Ofiti, N. O. E., Schmidt, M. W. I., Abiven, S., Hanson, P. J., Iversen, C. M., Wilson, R. M., Kostka, J. E., Wiesenberg, G. L. B., and Malhotra, A.: Climate warming and elevated CO_2 alter peatland soil carbon sources and stability, Nat. Commun., 14, 7533, https://doi.org/10.1038/s41467-023-43410-z, 2023.

Omar, M. S., Ifandi, E., Sukri, R. S., Kalaitzidis, S., Christanis, K., Lai, D. T. C., Bashir, S., and Tsikouras, B.: Peatlands in Southeast Asia: A comprehensive geological review, Earth-Sci. Rev., 232, 104149, https://doi.org/10.1016/j.earscirev.2022.104149, 2022.

Osaki, M., Kato, T., Kohyama, T., Takahashi, H., Haraguchi, A., Yabe, K., Tsuji, N., Shiodera, S., Rahajoe, J. S., Atikah, T. D., Oide, A., Matsui, K., Wetadewi, R. I., and Silsigia, S.: Basic Information About Tropical Peatland Ecosystems, in: Tropical Peatland Eco-management, edited by: Osaki, M., Tsuji,

N., Foead, N., and Rieley, J., Springer Singapore, Singapore, https://doi.org/10.1007/978-981-33-4654-3_1, 3–62, 2021.

Page, S. E., Rieley, J. O., and Banks, C. J.: Global and regional importance of the tropical peatland carbon pool, Glob. Change Biol., 17, 798–818, https://doi.org/10.1111/j.1365-2486.2010.02279.x, 2011.

Phillips, S. and Bustin, R. M.: Sedimentology of the Changuinola peat deposit: Organic and clastic sedimentary response to punctuated coastal subsidence, Geol. Soc. Am. Bull., 108, 794–814, https://doi.org/10.1130/0016-7606(1996)108<0794:SOTCPD>2.3.CO;2, 1996.

Phillips, S., Rouse, G. E., and Bustin, R. M.: Vegetation zones and diagnostic pollen profiles of a coastal peat swamp, Bocas del Toro, Panamá, Palaeogeogr. Palaeocl., 128, 301–338, https://doi.org/10.1016/S0031-0182(97)81129-7, 1997.

Petrenko, V. V., Severinghaus, J. P., Brook, E. J., Mühle, J., Headly, M., Harth, C. M., Schaefer, H., Reeh, N., Weiss, R. F., Lowe, D., and Smith, A. M.: A novel method for obtaining very large ancient air samples from ablating glacial ice for analyses of methane radiocarbon, J. Glaciol., 54, 233–244, https://doi.org/10.3189/002214308784886135, 2008.

R Core Team: R: A language and environment for statistical computing, R Foundation for Statistical Computing, Vienna, Austria, https://www.R-project.org/ (last access: 2 April 2025), 2022.

Ribeiro, K., Pacheco, F. S., Ferreira, J. W., De Sousa-Neto, E. R., Hastie, A., Krieger Filho, G. C., Alvalá, P. C., Forti, M. C., and Ometto, J. P.: Tropical peatlands and their contribution to the global carbon cycle and climate change, Glob. Change Biol., 27, 489–505, https://doi.org/10.1111/gcb.15408, 2021.

Sjögersten, S., Cheesman, A. W., Lopez, O., and Turner, B. L.: Biogeochemical processes along a nutrient gradient in a tropical ombrotrophic peatland, Biogeochemistry, 104, 147–163, https://doi.org/10.1007/s10533-010-9493-7, 2011.

Stuiver, M. and Polach, H. A.: Discussion Reporting of ^{14}C Data, Radiocarbon, 19, 355–363, https://doi.org/10.1017/S0033822200003672, 1977.

Sugimoto, A. and Wada, E.: Carbon isotopic composition of bacterial methane in a soil incubation experiment: Contributions of acetate and, Geochim. Cosmochim. Ac., 57, 4015–4027, https://doi.org/10.1016/0016-7037(93)90350-6, 1993.

Sun, C. L., Brauer, S. L., Cadillo-Quiroz, H., Zinder, S. H., and Yavitt, J. B.: Seasonal Changes in Methanogenesis and Methanogenic Community in Three Peatlands, New York State, Front. Microbiol., 3, 1–8, https://doi.org/10.3389/fmicb.2012.00081, 2012.

Thormann, M. N.: Diversity and function of fungi in peatlands: A carbon cycling perspective, Can. J. Soil Sci., 86, 281–293, https://doi.org/10.4141/S05-082, 2006.

Troxler, T. G.: Patterns of phosphorus, nitrogen and $\delta^{15}N$ along a peat development gradient in a coastal mire, Panama, J. Trop. Ecol., 23, 683–691, https://doi.org/10.1017/S0266467407004464, 2007.

Troxler, T. G., Ikenaga, M., Scinto, L., Boyer, J. N., Condit, R., Perez, R., Gann, G. D., and Childers, D. L.: Patterns of Soil Bacteria and Canopy Community Structure Related to Tropical Peatland Development, Wetlands, 32, 769–782, https://doi.org/10.1007/s13157-012-0310-z, 2012.

United Nations Environment Programme, Global Environment Facility, Asia Pacific Network for Global Change Research, Global Environment Centre (Malaysia), and Wetlands International (Eds.): Assessment on peatlands, biodiversity, and climate change, Global Environment Centre & Wetlands International, Wageningen, Kuala Lumpur, 2008.

Upton, A., Vane, C. H., Girkin, N., Turner, B. L., and Sjögersten, S.: Does litter input determine carbon storage and peat organic chemistry in tropical peatlands?, Geoderma, 326, 76–87, https://doi.org/10.1016/j.geoderma.2018.03.030, 2018.

Vogel, J. S., Southon, J. R., Nelson, D. E., and Brown, T. A.: Performance of catalytically condensed carbon for use in accelerator mass spectrometry, Nucl. Instrum. Meth. B, 5, 289–293, https://doi.org/10.1016/0168-583X(84)90529-9, 1984.

Wiesenberg, G. L. B., Dorodnikov, M., and Kuzyakov, Y.: Source determination of lipids in bulk soil and soil density fractions after four years of wheat cropping, Geoderma, 156, 267–277, https://doi.org/10.1016/j.geoderma.2010.02.026, 2010.

Wilson, R. M., Hopple, A. M., Tfaily, M. M., Sebestyen, S. D., Schadt, C. W., Pfeifer-Meister, L., Medvedeff, C., McFarlane, K. J., Kostka, J. E., Kolton, M., Kolka, R. K., Kluber, L. A., Keller, J. K., Guilderson, T. P., Griffiths, N. A., Chanton, J. P., Bridgham, S. D., and Hanson, P. J.: Stability of peatland carbon to rising temperatures, Nat. Commun., 7, 13723, https://doi.org/10.1038/ncomms13723, 2016.

Wilson, R. M., Griffiths, N. A., Visser, A., McFarlane, K. J., Sebestyen, S. D., Oleheiser, K. C., Bosman, S., Hopple, A. M., Tfaily, M. M., Kolka, R. K., Hanson, P. J., Kostka, J. E., Bridgham, S. D., Keller, J. K., and Chanton, J. P.: Radiocarbon Analyses Quantify Peat Carbon Losses With Increasing Temperature in a Whole Ecosystem Warming Experiment, J. Geophys. Res.-Biogeo., 126, e2021JG006511, https://doi.org/10.1029/2021JG006511, 2021.

Wright, E. L., Black, C. R., Cheesman, A. W., Drage, T., Large, D., Turner, B. L., and Sjögersten, S.: Contribution of subsurface peat to CO_2 and CH_4 fluxes in a neotropical peatland: CARBON FLUXES IN A NEOTROPICAL PEATLAND, Glob. Change Biol., 17, 2867–2881, https://doi.org/10.1111/j.1365-2486.2011.02448.x, 2011.

Wright, E. L., Black, C. R., Turner, B. L., and Sjögersten, S.: Environmental controls of temporal and spatial variability in CO_2 and CH_4 fluxes in a neotropical peatland, Glob. Change Biol., 19, 3775–3789, https://doi.org/10.1111/gcb.12330, 2013.

Zhang, Y., Ma, A., Zhuang, G., and Zhuang, X.: The acetotrophic pathway dominates methane production in Zoige alpine wetland coexisting with hydrogenotrophic pathway, Sci. Rep., 9, 9141, https://doi.org/10.1038/s41598-019-45590-5, 2019.